Title

An Oxidative Central Metabolism Enables Salmonella to Utilize Microbiota-Derived Succinate

Journal

Cell Host & Microbe, 22(3)

ISSN

1931-3128

Authors

Spiga, Luisella
Winter, Maria G
de Carvalho, Tatiane Furtado
et al.

Publication Date

2017-09-01

DOI

10.1016/j.chom.2017.07.018

Peer reviewed

HHS Public Access

Author manuscript

Cell Host Microbe. Author manuscript; available in PMC 2018 September 13.

Published in final edited form as:

Cell Host Microbe. 2017 September 13; 22(3): 291–301.e6. doi:10.1016/j.chom.2017.07.018.

An oxidative central metabolism enables *Salmonella* to utilize microbiota-derived succinate

Luisella Spiga[1,*], **Maria G. Winter**[1,*], **Tatiane Furtado de Carvalho**[2], **Wenhan Zhu**[1], **Elizabeth R. Hughes**[1], **Caroline C. Gillis**[1], **Cassie L. Behrendt**[3], **Jiwoong Kim**[4], **Daniela Chessa**[5], **Helene L. Andrews-Polymenis**[6], **Daniel P. Beiting**[7], **Renato L. Santos**[2], **Lora V. Hooper**[3,8], and **Sebastian E. Winter**[1]

[1]Department of Microbiology, UT Southwestern Medical Center, Dallas, TX 75390, USA

[2]Departamento de Clínica e Cirurgia Veterinárias, Escola de Veterinária, Universidade Federal de Minas Gerais, Belo Horizonte, MG, Brazil

[3]Department of Immunology, UT Southwestern Medical Center, Dallas, TX 75390, USA

[4]Department of Clinical Science, Quantitative Biomedical Research Center, UT Southwestern Medical Center, Dallas, TX 75390, USA

[5]Department of Biomedical Science, School of Medicine, University of Sassari, Sassari, Italy

[6]Department of Microbial Pathogenesis and Immunology, College of Medicine, Texas A&M University System Health Science Center, Bryan, TX 77807, USA

[7]Department of Pathobiology, School of Veterinary Medicine, University of Pennsylvania, Philadelphia, PA 19104, USA

[8]Howard Hughes Medical Institute, UT Southwestern Medical Center, Dallas, TX 75390, USA

SUMMARY

The mucosal inflammatory response induced by *Salmonella* Typhimurium creates a favorable niche for this gut pathogen. Conventional wisdom holds that *S.* Typhimurium undergoes an incomplete TCA cycle in the anaerobic mammalian gut. One change during *S.* Typhimurium-induced inflammation is the production of oxidized compounds by infiltrating neutrophils. We show that inflammation-derived electron acceptors induce a complete, oxidative TCA cycle in *S.* Typhimurium, allowing the bacteria to compete with the microbiota for colonization. A complete TCA cycle facilitates utilization of the microbiota-derived fermentation end product succinate as a carbon source. *S.* Typhimurium succinate utilization genes contribute to efficient colonization in

Lead Contact: Sebastian.Winter@UTSouthwestern.edu.

*Authors contributed equally

AUTHOR CONTRIBUTIONS

SEW, LVH, DC, HAP, DPB, and RLS designed and conceived the study; LS, MGW, WZ, ERH, CCG, CLB, and SEW performed all experiments. RLS and TFC performed the histopathology analysis. WZ, DPB, and JK generated and analyzed the RNAseq data. All authors contributed to data analysis and writing the manuscript.

conventionally raised mice, but provide no growth advantage in germ-free mice. Mono-association of gnotobiotic mice with *Bacteroides,* a major succinate producer, restores succinate utilization in *S*. Typhimurium. Thus, oxidative central metabolism enables *S*. Typhimurium to utilize a variety of carbon sources, including microbiota-derived succinate.

eTOC BLURB

Spiga, *et al*. show that during colonization of the intestinal lumen, the enteric pathogen *S*. Typhimurium performs a complete TCA cycle. This oxidative central metabolism enables *S*. Typhimurium to utilize the microbiota-derived fermentation product succinate as a nutrient and to compete with the microbiota for colonization of the intestinal tract.

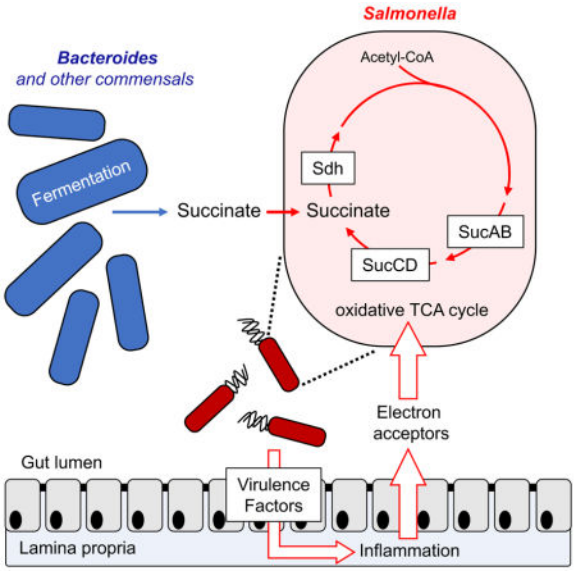

INTRODUCTION

The bacterial species dominating the microbiota in the large bowel are obligate anaerobic bacteria belonging to the phyla Bacteroidetes (class Bacteroidia) and Firmicutes (class Clostridia). With amino acids and simple sugars being absorbed in the small intestine, the primary carbon and energy sources for obligate anaerobic bacteria in the large intestine are complex glycans of dietary and host origin (reviewed in (Fischbach and Sonnenburg, 2011; Flint et al., 2012; Koropatkin et al., 2012; Martens et al., 2014)). Glycan degradation by the starch utilization system (*sus*) machinery has been studied extensively in obligate anaerobic commensal *Bacteroides* spp.. The genomes of sequenced *Bacteroides* strains are predicted to encode a large variety of distinct, *sus*-like systems that allow the utilization of a plethora of structurally unrelated glycans (Cuskin et al., 2015; El Kaoutari et al., 2013; Rogowski et al., 2015; Xu et al., 2003), with different *Bacteroides* strains exhibiting preference for distinct glycans (Pudlo et al., 2015). Similarly, commensal *Bifidobacterium* spp. and *Clostridia* produce extracellular glycoside hydrolases and other carbohydrate-active enzymes, allowing the fermentation of complex polysaccharides (Crost et al., 2013; El Kaoutari et al., 2013; Schell et al., 2002; Schwarz et al., 2004; Shimizu et al., 2002). Glycan degradation by

Clostridia and Bacteroidia generates primary fermentation end products, which support the growth of syntrophic bacteria and archaea as minor constituents of the gut microbiota (Macy et al., 1975; Turton et al., 1983). Collectively, the ability to degrade a variety of complex polysaccharides directly correlates with the overall abundance of commensal gut microbes in the ecosystem (Eilam et al., 2014), indicating that polysaccharide utilization is a major determinant of the microbiota composition in the healthy gut.

Curiously, infection with enteric pathogens disturbs the normal gut microbiota structure, culminating in a bloom of the luminal pathogen population (Barman et al., 2008; Lupp et al., 2007; Stecher et al., 2007). Increased bacterial colonization of the intestinal tract enhances transmission success of the pathogen by the fecal oral route (Lawley et al., 2008; Rivera-Chavez et al., 2016). Proteobacteria express a very limited number of secreted glycoside hydrolases (El Kaoutari et al., 2013), suggesting that the metabolic pathways that allow gut colonization of pathogenic Enterobacteriaceae such as *Salmonella enterica* serotype Typhimurium (*S.* Tm; Phylum Proteobacteria, Family Enterobacteriaceae) must be different from the glycan-foraging mechanisms utilized by commensal Bacteroidia and Clostridia.

Several mechanisms have been shown to enhance fitness of *S.* Tm in the inflamed gut. Modifications of the outer membrane confer resistance to antimicrobial peptides and bile (Crawford et al., 2012; Gunn, 2008). To overcome nutritional immunity, siderophores facilitate the uptake of micronutrients such as iron and zinc (Liu et al., 2012; Raffatellu et al., 2009). Byproducts of reactive nitrogen and oxygen species generated in the wake of the host inflammatory are utilized as respiratory electron acceptors (Lopez et al., 2012; Winter et al., 2010). Furthermore, inflammation-associated changes in the colonocyte metabolism include leakage of molecular oxygen into the lumen, which supports oxygen respiration in *S.* Tm through high-affinity terminal oxidases (Rivera-Chavez et al., 2016). Utilization of microbiota-derived molecular hydrogen enhances initial colonization of the intestinal tract by *S.* Tm (Maier et al., 2013). While colonization of the inflamed gut by *S.* Tm has been studied extensively, the adaptation of the central metabolism to the nutritional environment of the inflamed intestine has not been elucidated. Here, we investigated the tricarboxylic acid (TCA) cycle as part of the central intermediary metabolism in the enteric pathogen *S.* Tm in an inbred mouse model of infection.

RESULTS

Contribution of TCA cycle enzymes to fitness of *S.* Tm in the streptomycin-treated mouse model

Current dogma holds that Enterobacteriaceae and many other bacteria do not express α-ketoglutarate dehydrogenase (SucAB), succinyl-CoA synthetase (SucCD), and succinate dehydrogenase (Sdh) under anaerobic conditions, resulting in a bifurcation of the TCA into a reductive and oxidative branch (Fig. 1A) (Amarasingham and Davis, 1965; Cronan and Laporte, 2013; Iuchi and Lin, 1988). In this arrangement, biosynthetic reactions of the TCA cycle can still occur, but acetyl-CoA cannot be oxidized. Surplus reduction equivalents are used to reduce the internal terminal electron acceptor fumarate. Based on these considerations, one would assume that the TCA cycle of *S.* Tm in the gut lumen is branched and α-ketoglutarate dehydrogenase, succinyl-CoA synthetase, and Sdh activity is

dispensable (Fig. 1A). To test this idea, we generated a *S.* Tm mutant lacking the major subunit of Sdh (Δ*sdhA*) and determined fitness in a murine model of *Salmonella*-induced colitis (Fig. 1B – D; Fig. S1). Groups of streptomycin-treated C57BL/6 mice (Barthel et al., 2003) were intragastrically inoculated with an equal mixture of the *S.* Tm wild-type strain (AJB715), and an Δ*sdhA* mutant, or mock-treated. Four days after infection, the bacterial load for each strain was determined in the colonic and cecal content by plating on selective media and the ratio of wild-type strain bacteria to mutant bacteria (competitive index) calculated (Fig. 1C and D). Interestingly, the *S.* Tm wild-type strain was recovered in higher numbers than the Δ*sdhA* mutant, suggesting that Sdh activity was required for efficient colonization of the gut during infection.

Since the TCA cycle is an essential component for the intermediary metabolism, we were concerned that TCA cycle mutants were generally impaired for growth. We therefore sought to determine the fitness of TCA cycle mutants in the absence of inflammation. *S.* Tm employs two type three secretion systems to invade non-phagocytic epithelial cells and to mediate replication in the mucosa, respectively (Galan and Curtiss, 1989; Hensel et al., 1998). Mutants lacking both type three secretion systems (T3SS1/2; Δ*invA* Δ*spiB*) do not induce overt inflammatory responses (Fig. 1B and Fig. S1A – C) and colonize the gut lumen to a limited extent (Coombes et al., 2005; Hapfelmeier et al., 2004; Hapfelmeier et al., 2005). The T3SS1/2 and the T3SS1/2 Δ*sdhA* mutants were recovered in similar numbers (Fig. 1C and D), indicating that Sdh activity is dispensable in the absence of inflammatory responses. These experiments raised the possibility that *S.* Tm uses a complete TCA cycle during infection.

Exogenous electron acceptors impact the *S.* Tm TCA cycle *in vitro* and *in vivo*

Addition of the alternative electron acceptor nitrate to anaerobic culture media can induce expression of TCA cycle enzymes in *E. coli* K-12, however this phenomenon only occurs in the absence of the regulatory protein ArcA (Perrenoud and Sauer, 2005; Prohl et al., 1998; Wimpenny and Cole, 1967). During mucosal inflammation, alternative electron acceptors such as nitrate and tetrathionate occur as byproducts of the oxidative burst (Winter et al., 2010). To test whether alternative electron acceptors could influence the TCA cycle in *S.* Tm, we cultured mixtures of the *S.* Tm wild-type strain and isogenic mutants deficient in TCA cycle enzymes in mucin broth under anaerobic conditions for 16 h. The wild-type strain outcompeted the Δ*sucAB,* Δ*sucCD,* and Δ*sdhA* mutant when nitrate or tetrathionate was added to the growth media while no growth advantage was apparent in the absence of exogenous electron acceptors (Fig. 1E – G). This outcome indicated that alternative electron acceptors are sufficient to alter operation of the TCA cycle in *S.* Tm.

Next, we investigated whether nitrate and tetrathionate increase transcription of *sucA* and *sdhA* during anaerobic growth in mucin broth. RNA was extracted after 16 h and *sucA* and *sdhA* mRNA levels were determined by RT-qPCR (Fig. 2A and B). Transcription of *sucA* and *sdhA* increased significantly in the presence of alternative electron acceptors. We then determined the transcriptome of *S.* Tm during colonization of the intestinal tract (Fig. S2). To this end, we colonized gnotobiotic mice with the *S.* Tm wild-type strain and performed RNAseq on RNA extracted from cecal content. A comparison to a published transcriptome

database of *S*. Tm cultured in various *in vitro* conditions (Kroger et al., 2013) showed that the *in vivo* transcriptome formed a state distinct from all *in vitro* conditions in the database (Fig. S2A). To assess the overall metabolic state, we compared normalized mRNA levels of selected metabolic enzymes under aerobic and anaerobic culture conditions *in vitro* and in the mouse model (Fig. S2B – G). Transcription of general housekeeping enzymes such as glyceraldehyde-3-phosphate dehydrogenase (*gapA*), acetate kinase (*ackA*), and phosphate acetyltransferase (*pta*) was comparable in all three conditions (Fig. S2B). Consistent with the notion that nitrate and tetrathionate are inducers of the respective reductase operons (Hensel et al., 1999; Rabin and Stewart, 1993), transcription of the tetrathionate reductase, nitrate reductase-1, and the periplasmic nitrate reductase in the murine cecum was increased compared to standard aerobic and anaerobic *in vitro* conditions (Fig. S2C – E). Furthermore, transcription of *sucAB*, *sucCD*, and *sdh* in the murine model was found to be most similar to growth under aerobic *in vitro* conditions (Fig. S2F), which was suggestive of an overall oxidative central metabolism in *S*. Tm during gut colonization.

We then explored whether inflammation alters expression of key TCA cycle enzymes in the streptomycin-treated mouse model (Fig. 2C – F). A marked increase in pro-inflammatory markers was observed three days after infection (Fig. 2D and Fig. S1C). Low levels of inflammation were noted early during infection with the wild-type strain (2 days after infection; Fig. 2C) and when mice were infected with a T3SS1/2-deficient mutant (Fig. 2C and 2D). Transcription of *sdhA* and *sucA* in the *S*. Tm wild-type strain and the T3SS1/2-deficient mutant were similar two days after infection (Fig. 2E). Concomitant with the onset of inflammation three days after infection, the wild-type strain exhibited a significant increase in *sdhA* and *sucA* mRNA levels compared to the ΔT3SS1/2 mutant (Fig. 2F), indicating that increased levels of mucosal inflammation correlates with increased expression of *S*. Tm TCA cycle enzymes.

During *Salmonella* infection, neutrophils infiltrating the mucosa undergo an oxidative burst with the release of reactive oxygen (ROS) and nitrogen species (RNS) (Fig. 3A). NADPH oxidase 2 (NOX2, PHOX), comprised of the two chains CYBA and CYBB, catalyzes the first step in the generation of ROS. Inducible nitric oxide synthase (iNOS) is the sole source of nitric oxide. Oxidation of thiosulfate by ROS yields tetrathionate in the gut lumen (Winter et al., 2010) while peroxide can react with nitric oxide to form peroxynitrite, a reactive nitrogen species that decomposes to nitrate (Winter et al., 2013). To assess whether availability of tetrathionate and nitrate affects the *S*. Tm TCA cycle during infection, we repeated the competitive colonization assay in NOX2 (*Cybb*)- and iNOS (*Nos2*)-deficient mice. In heterozygous $Cybb^{+/-}$ littermate controls, the *S*. Tm wild-type strain outcompeted the *sdhA* mutant, while this competitive fitness advantage was abrogated in homozygous *Cybb*-deficient animals (Fig. 3B). The fitness advantage conferred by Sdh activity was significantly reduced in *Nos2*-deficient mice but not completely abrogated as in the *Cybb*-deficient mice suggesting that both tetrathionate and nitrate likely contribute to changes in the central metabolism of *S*. Tm *in vivo* (Fig. 3C). During *S*. Tm infection, butyrate-producing *Clostridia* spp. are diminished from the gut microbiota (Rivera-Chavez et al., 2016). Depletion of butyric acid, the main carbon source of intestinal epithelial cells, causes a perturbation in the epithelial metabolism and small amounts of oxygen become available at the mucosal interface. Thus, we considered the possibility that, in addition to nitrate and

tetrathionate, molecular oxygen could influence the direction of the TCA cycle in the mammalian gut lumen. Supplementation with tributyrin, a source of butyrate that prevents oxygen leakage into the gut lumen (Rivera-Chavez et al., 2016), moderately reduced the competitive fitness of the wild-type strain over the *sdhA* mutant (Fig. 3C). Collectively, these data suggest that availability of exogenous electron acceptors, such as nitrate, tetrathionate, and oxygen, alter the central metabolism of *S*. Tm in a mouse model of infection.

A complete TCA cycle enhances *S*. Tm fitness in competition with the native microbiota

To determine whether a complete TCA cycle might enhance fitness of *S*. Tm in competition with the unperturbed, native gut microbiota, we used CBA mice. CBA mice develop neutrophilic inflammation of the large intestine after 7 to 10 days (Fig. S3A and B). The competitive fitness of the *S*. Tm wild-type strain and mutants lacking TCA cycle enzymes was determined 7 days after infection (Fig. 4A and B). The *S*. Tm wild-type strain outcompeted the Δ*sucAB*, Δ*sucCD*, and Δ*sdhA* mutants. The glyoxylate shunt, a pathway bypassing α-ketoglutarate dehydrogenase and succinyl-CoA synthetase, was dispensable for growth in the inflamed gut since a Δ*aceAB* mutant did not exhibit a fitness defect under the conditions tested (Fig. 4A and B). Sdh activity did not confer a fitness advantage in the absence of inflammation (Δ*invA* Δ*spiB* mutant background) in the CBA mouse model. Complementation of the *sdhA* mutant by introducing the *sdhA* promoter and coding sequence into the neutral *phoN* recapitulated the phenotype of the wild-type strain (Fig. 4A and B). Similar observations were made using another *S*. Tm isolate, SL1344 (Fig. S3C).

To determine whether a complete TCA cycle contributed to growth of *S*. Tm in direct competition with the native microbiota, we infected groups of CBA animals intragastrically with either the *S*. Tm wild-type strain or the Δ*sdhA* mutant (single infection). Both strains induced host inflammation to a similar degree (Fig. 4C and D; Fig. S3). However, the *sdhA*-deficient mutant was recovered at significantly lower numbers than the wild-type strain in the cecum and colon content (29-fold and 80-fold, respectively) 7 days after infection (Fig. 4E and F). Collectively, the experiments support for the idea that switching from a branched to a full TCA cycle is a critical metabolic adaption for *S*. Tm to compete with the native microbiota for colonization of the intestinal tract.

Utilization of dicarboxylic acids by *S*. Tm

One potential consequence of the inflammation-associated oxidative central metabolism of *S*. Tm could be that poorly fermentable dicarboxylic acids, such as succinate, could serve as carbon sources by feeding directly into the TCA cycle. To test if uptake of di- and tri-carboxylic acids contributes to growth of *S*. Tm during colitis, we constructed mutants lacking the C4-dicarboxylate carriers DctA (succinate-proton symporter), DcuA (succinate-proton symporter), and DcuB (fumarate-succinate antiporter) (Δ*dcuA* Δ*dcuB* Δ*dctA* mutant; Δ3 mutant). In CBA mice, the *S*. Tm wild-type strain outcompeted the Δ3 mutant by a 5-fold (Fig. 5A). Similarly, the Δ3 mutant exhibited a gut colonization defect compared to the wild-type strain in single infection experiments (Fig. 5B and C), indicating that C4-dicarboxylate uptake enhances fitness of *S*. Tm in the lumen of the mammalian intestine.

Microbiota-derived succinate supports growth of *S*. Tm during infection

Obligate anaerobic commensals, in particular *Bacteroides* spp., use a branched TCA cycle to support fumarate respiration. The end product of fumarate reduction, succinate, is secreted into the extracellular environment. In the human gut, luminal succinate levels are ranging from approximately 0.5 to 5 mM (Cummings et al., 1987; Meijer-Severs and van Santen, 1987; Rubinstein et al., 1969). In the CBA mouse model, the concentration of succinate was found to be about 0.4 mM in the cecum content and 3 mM in the colon content (Fig. 5D and E). No changes in extracellular succinate levels upon *S*. Tm infection were noted. Based on these findings, we hypothesized that *Bacteroides*-derived succinate could be utilized by *S*. Tm as a consequence of a complete TCA cycle. To investigate this idea, we cultured *B. thetaiotaomicron* in mucin broth for 3 days. Growth of *B. thetaiotaomicron* lead to the accumulation of succinate in the filter-sterilized culture supernatant (Fig. 6A). Next, we determined anaerobic growth of *S*. Tm using the *B. thetaiotaomicron*-fermented mucin as a growth media. In the absence of any exogenous electron acceptor, C4-dicarboxylate transporters did not provide a growth advantage. However, when nitrate was added to the media to switch from a branched to a complete TCA cycle, the wild-type strain outcompeted the Δ*dcuA* Δ*dcuB* Δ*dctA* mutant (Fig. 6B).

C4-dicarboxylate transporters can facilitate the uptake of succinate and several other dicarboxylates, such as fumarate, aspartate, malate, and tartrate (reviewed in (Unden and Kleefeld, 2004)). In the absence of Sdh activity (Δ*sdhA* vs. Δ*sdhA* Δ3 mutant), the growth advantage conferred by C4-dicarboxylate transporters was abolished supporting the notion that the growth advantage conferred by these uptake systems was indeed due to succinate uptake. (Fig. 6B). Collectively, these experiments demonstrate that *B. thetaiotaomicron*-derived succinate can be utilized by *S*. Tm in the presence of exogenous electron acceptors *in vitro*.

Next, we investigated succinate uptake and utilization in gnotobiotic mice (genetically resistant Swiss Webster mice) and mice that had been mono-associated with *B. thetaiotaomicron*. Infection with *S*. Tm induced significant pathological changes in the cecal and colonic mucosa in both groups (Fig. 6C; Fig. S4 and S5A and B). Consistent with the idea that succinate is derived from the gut microbiota, C4-dicarboxylate uptake (Δ3 mutant) and Sdh activity (Δ*sdhA* mutant) were dispensable for intestinal colonization during infection of gnotobiotic mice (Fig. 6D and E; Fig. S5C). Importantly, mono-colonization with *B. thetaiotaomicron* was sufficient to reinstate the fitness advantage conferred by C4-dicarboxylate uptake (Fig. 6D and E; Fig. S5C). In the absence of succinate degradation (Δ*sdhA vs.* Δ*sdhA* Δ3), the effect of C4-dicarboxylate uptake on competitive fitness was minimal in the gnotobiotic mouse model as well as in conventionally-raised CBA mice (Fig. 5A; Fig. 6D and E). We also generated a *B. thetaiotaomicron* that is unable to generated succinate *in vitro* and *in vivo* (Fig. S6A and B) due to a lack of fumarate reductase activity (Δ*frd*). In contrast to the *B. thetaiotaomicron* wild-type strain, mono-association with the *B. thetaiotaomicron* Δ*frd* mutant was unable to restore the fitness advantage C4-dicarboxylate uptake in *S*. Tm (Fig. 6D and E). Metabolic profiling of large intestinal contents of mice mono-associated with the *B. thetaiotaomicron* wild-type strain and the isogenic Δ*frd* mutant revealed an absence of succinate in Δ*frd* colonized mice (Fig. S6B and C) and a

compensatory increase in lactate levels (Fig. S6C). Lactate is not known to be transported by C4-dicarboxylate carriers and does not serve as a substrate for Sdh. Collectively, these experiments demonstrate that microbiota-derived succinate is taken up and is utilized by *S.* Tm during colonization of the inflamed intestinal tract.

DISCUSSION

The central metabolism of *S.* Tm has been analyzed extensively *in vitro* and in murine models of systemic infection. *S.* Tm mutants lacking key TCA cycle enzymes are defective for replication in tissue at systemic sites (Mercado-Lubo et al., 2008; Mercado-Lubo et al., 2009; Tchawa Yimga et al., 2006). TCA cycle reactions are predicted to have high metabolic conversion rates during growth in the spleen (Steeb et al., 2013). Furthermore, the central metabolism of *S.* Tm shapes host-microbe interactions during infection of macrophages. A complete, oxidative TCA cycle is of critical importance for *S.* Tm to avoid pyroptotic cell death in macrophages in cell culture (Wynosky-Dolfi et al., 2014). Activated macrophages restrict bacterial metabolism by releasing reactive nitrogen species to deactivate the lipoamide-dependent enzymes pyruvate and α-ketoglutarate dehydrogenase (Richardson et al., 2011). Infection of immune-competent individuals with non-typhoidal *Salmonella* serotypes results in a self-limiting gastroenteritis and no bacterial dissemination is observed. Curiously, the central metabolism of *S.* Tm during natural infection, i.e. during *Salmonella*-induced colitis, has not been investigated.

Strict anaerobic commensals have evolved to successfully compete for carbon and energy sources in the nutrient-limiting environment of the healthy large intestine. As a combined function of the metabolism of the bacterial community, all energetically valuable compounds are depleted, hampering intrusion of the ecosystem by enteric pathogens. To overcome this colonization resistance, *S.* Tm triggers an acute mucosal inflammatory response, which creates a niche in the lumen of the intestine that is suitable for the outgrowth of *S.* Tm over other commensals (Barman et al., 2008; Stecher et al., 2007). One prominent change in the gut environment during *S.* Tm infection is the production of oxidized compounds such as nitrate and tetrathionate as byproducts of the oxidative burst by infiltrating neutrophils (Lopez et al., 2012; Winter et al., 2010). Unlike obligate anaerobic commensals, *S.* Tm utilizes these oxidized compounds as electron acceptors for the electron transport chain. Here we show mucosal inflammation significantly alters the central metabolism of the *S.* Tm population residing in the gut lumen. Alternative electron acceptors, such as nitrate, change the direction of the TCA from a branched set of reactions to a full, oxidative TCA cycle in the mammalian intestine.

An oxidative central metabolism could enhance growth of *S.* Tm through several mechanisms. Carbon sources that are fully or partially degraded to acetyl-CoA could enter the TCA cycle and be oxidized to CO_2 *in vivo. In vitro*, *Salmonella* is known to utilize a great variety of compounds as the sole carbon source during aerobic conditions (Gutnick et al., 1969). In the murine gut, only few carbon sources have been identified, such as ethanolamine, 1,2 propanediol, and fructose-asparagine (Ali et al., 2014; Faber et al., 2017; Thiennimitr et al., 2011). An oxidative TCA cycle may explain why utilization of these compounds *in vivo* strictly requires respiration. In this study, we demonstrate that C4-

dicarboxylic acids may serve as nutrients for *S*. Tm during infection. Specifically, uptake and utilization of succinate, enhances *S*. Tm growth in the inflamed gut. Succinate is generated as a predominant fermentation end product of Bacteroides in the reductive branch of a split TCA cycle. During inflammation, this metabolism is mirrored by *S*. Tm as the set of reactions that make up the reductive branch is reversed. This metabolic adaptation to the inflamed gut allows the pathogen to utilize a microbiota-derived metabolic waste product as a nutrient.

Since the phenotype of the C4-dicarboyxlate uptake mutant only partially recapitulated the phenotype of the *sdhA* mutant, it is likely that the oxidative TCA cycle enhances *S*. Tm fitness by additional mechanisms. For example, in *Proteus mirabilis*, an oxidative TCA cycle is required to generate energy for swarming (Alteri et al., 2012). Flagella-mediated motility is required for *S*. Tm to efficiently colonize the inflamed gut lumen (Stecher et al., 2008). Furthermore, it is possible that other carbon sources could enter the oxidative TCA cycle, either as acetyl-CoA or through anaplerotic reactions. Of note, the phenotype of the C4-dicarboyxlate uptake mutant was not entirely abolished during infection in gnotobiotic mice, suggesting that dietary or host-derived C4-dicarboyxlates might be utilized by *S*. Tm as well. Collectively, an oxidative TCA cycle might give *S*. Tm flexibility in nutrient acquisition and energy generation during colonization of the gastrointestinal tract.

Apart from serving as a nutrient, succinate acts as a cue for some enteric pathogens. Expression of the Locus of Enterocyte Effacement (LEE), a major virulence factor of Enterohemorrhagic *E. coli*, is regulated *in vivo* by succinate (Curtis et al., 2014). Furthermore, oral antibiotic therapy is associated with blooms of *C. difficile*. In mouse models, an antibiotic-induced perturbation of the microbiota increases the local availability of succinate, which in return supports the expansion of *C. difficile* (Ferreyra et al., 2014). Our work shows that microbiota-derived succinate fuels *S*. Tm growth during natural infection without the need for antibiotic treatment, thus identifying a critical microbiota-pathogen interaction in the context of infection of the mammalian host.

STAR METHODS

CONTACT FOR REAGENT AND RESOURCE SHARING

Further information and requests for resources and reagents should be directed to and will be fulfilled by the Lead Contact, Sebastian E. Winter (Sebastian.Winter@UTSouthwestern.edu).

EXPERIMENTAL MODEL AND SUBJECT DETAILS

Mice—C57BL/6, *Cybb*-deficient (on the C57BL/6 background), *Nos2*-deficient (on the C57BL/6 background) and CBA mice were originally obtained from the Jackson Laboratory and bred at UT Southwestern. Germ-free Swiss Webster mice were maintained in specific pathogen-free facilities at UT Southwestern Medical Center. Some of the germ-free mice were colonized with CBA mice microbiota to obtain the Swiss Webster mice used in this study. Conventional mice were housed in individually ventilated cages with *ad libitum* access to water and feed (Envigo Global 16% Protein Rodent Diet). The age at the begin of

the experiment was 7–10 weeks for C57BL/6 WT, *Cybb*, and *Nos2*-deficient mice, 8–10 weeks for CBA mice, and 6–8 weeks for Swiss Webster mice. Unless indicated otherwise in the figure legend, both male and female mice were analyzed and no significant sex-specific differences were noted. Both sexes were equally represented in each experimental group.

Animals were randomly assigned into cages and treatment groups 3 days prior to experimentation. Unless stated otherwise, a minimum of 5 mice were used based on variability observed in previous experiments. At the end of the experiments, mice were humanely euthanized using carbon dioxide inhalation. Animals that had to be euthanized for humane reasons prior to reaching the predetermined time point were excluded from the analysis. All experiments involving mice were approved by the Institutional Animal Care and Use Committee at UT Southwestern Medical Center (APN# T-2013-0139, T2014-0061, T-2015-0031).

Bacterial culture—*E. coli* and *S.* Tm strains were routinely grown aerobically at 37°C in LB broth (10 g/l tryptone, 5 g/l yeast extr act, 10 g/l sodium chloride) or on LB agar plates (10 g/l tryptone, 5 g/l yeast extract, 10 g/l sodium chloride, 15 g/l agar). *B. thetaiotaomicron* strains were routinely cultured on blood agar plates (37 g/l brain heart infusion medium, 15 g/l agar, 50 ml sheep blood, 50 mg/l glutamine), Columbia blood plates (42 g/l Columbia agar, 5 % [v/v] defibrinated blood, 5 mg/l hemin, 0.02% [v/v] of a 0.5 % [v/v] Vitamin K1 solution in 95 % ethanol), or in modified TYG broth (10 g/l tryptone, 5 g/l yeast extract, 2 g/l glucose, 0.5 g/l cysteine 0.1 M potassium phosphate pH 7.2, 1 mg/l Vitamin K, 0.02 g/l magnesium sulfate heptahydrate, 0.4 g/l sodium bicarbonate, 0.08 g/l sodium chloride, 8 mg/l calcium chloride, 0.4 mg/l iron (II) sulfate, 1 mg/l resazurin, 40 μM histidine, 2.4 μg/l hematin) in an anaerobic chamber (Sheldon Manufacturing; 5 mol % H_2, 5 % CO_2, 90 % N_2). When appropriate, agar plates and media were supplemented with 30 μg/ml chloramphenicol (Cm), 100 μg/ml carbenicillin (Carb), 50 μg/ml kanamycin (Kan), 50 μg/ml nalidixic acid (Nal), 50 μg/ml gentamycin (Gent), 25 μg/ml erythromycin (Erm), 25 μg/ml tetracycline (Tet) or 200 μg/ml 5-fluoro-2′-deoxyuridine (FUdR). For competitive growth assays, diluted samples were spread onto agar plates containing the chromogenic substrate 5-bromo-4-chloro-3-indolyl phosphate (40 mg/l) to detect acidic phosphatase (PhoN) activity. The competitive index was calculated by dividing the number of wild-type bacteria by the number of mutant bacteria in the output, divided by the same ratio obtained from the inoculum.

METHOD DETAILS

Construction of plasmids—To generate pSW284, pSW286 and pSW288, the upstream and downstream regions of *S.* Tm IR715 *sucAB*, *sucCD* and *aceAB* were amplified by PCR using the primer sets listed in the table below. Purified PCR products were digested with XbaI and ligated with T4 DNA ligase. The joint upstream and downstream regions were then amplified by PCR using the outside primers and cloned into pCR2.1. The DNA sequence of the cloned PCR product was verified by Sanger sequencing. The DNA fragment was subcloned into pRDH10 using BamHI and SalI restriction sites. To construct pSW306, pSW300, pSW301, and pSW299, the upstream regions of *sdhA, dcuA dcuB,* and *dctA* were PCR amplified from the IR715 chromosome. Purified PCR products and purified, SphI-

digested pRDH10 were ligated using the Gibson cloning procedure in a three-part ligation. The DNA sequence of the upstream and downstream region was determined sequencing. For pSW328, an internal fragment of the *phoN* coding sequence was amplified by PCR and cloned into SacI-digested pGP704 in a Gibson cloning reaction. Subsequently, the promoter and coding sequence of the *S*. Tm *sdh* operon were amplified and cloned into the SphI restriction enzyme site of pSW327. To generate pMW5, regions upstream and downstream of *frdCAB* in *B. thetaiotaomicron* were PCR amplified and the products were inserted into the BamHI site of the suicide vector pExchange-tdk through Gibson assembly. The cloning strain for all suicide plasmids was DH5α λ*pir*.

Generation of *S*. Tm mutants—Suicide plasmids were introduced into *S*. Tm by conjugation using S17-1 λ*pir* as the donor strain. For pRDH10 and pGP704 derivatives, Cm and Carb, respectively were used to select for single cross over events. To select for a second crossover event, sucrose selection was performed (Lawes and Maloy, 1995). pSW306, pSW284, pSW286, pSW288 were used generate SW1397, SW1285, SW1286, SW1288 in the IR715 background and to generate MW156 in the SL1344 background, respectively. pSW328 was integrated into SW1397 to give rise to SW1410. Integration of pSW328 into the *phoN* gene was confirmed by PCR and lack of acidic phosphatase activity. SW1411 was generated by sequential introduction of pSW299, pSW300, and pSW301 into IR715 followed each time by sucrose selection. The *phoN*::Kan^R mutation was transduced by phage P22 HT *int-105* (Schmieger, 1972) from AJB715 into SPN487 and SW1397 to generate SW1401 and SW1414, respectively. Similarly, the Δ*sdhA*::Kan^R from STM0734 was introduced into IR715, SPN487 and SW1411, thus generating SW1056, SW1203 and SW1413, respectively. To create MW231, the Δ*invA*::Tet^R and Δ*spiB*::Kan^R mutations from SPN452 were transduced separately. Introduction of phoN::CmR and pSW306 into MW231 produced MW251 and MW256, respectively.

Construction of a *B. thetaiotaomicron frd* mutant—MW399, an isogenic derivative of the *B. thetaiotaomicron* strain ATCC 29148 Δ*tdk* deficient for *frdCAB,* was generated via allelic exchange (Koropatkin et al., 2008). pMW5 was introduced into ATCC 29148 Δ*tdk* via bacterial conjugation with the donor strain S17-1 λ*pir*. The conjugation was carried out on blood plates under aerobic conditions at 37°C to enable the growth of the S17-1 λ*pir* strain. All further steps were performed under anaerobic conditions to insure proper growth of the *B. thetaiotaomicron* strains. Exconjugates in which the suicide plasmid had integrated into the chromosome by single crossover were selected for on blood plates containing Gent and Erm. Then, the second homologous recombination event was selected for on blood plates containing FUdR. The second crossover event leads to an unmarked deletion of *frdCAB*, which was confirmed by PCR. The growth media was routinely supplemented with hemin.

Growth of Bacteroides thetaiotaomicron in mucin broth—Porcine mucin was sterilized by suspending 100 mg in 1 ml of 70 % ethanol for 24 h. The ethanol was removed by drying in a vacuum concentrator. Sterile mucin was dissolved in No-Carbon E medium (NCE) (3.94 g/l monopotassium phosphate, 5.9 g/l dipotassium phosphate, 4.68 g/l ammonium sodium hydrogen phosphate tetrahydrate, 2.46 g/l magnesium sulfate

heptahydrate) at a final concentration of 0.5 % (w/v). Mucin broth was inoculated with a fresh colony of *Bacteroides thetaiotaomicron* and incubated under anaerobic conditions for 72 h at 37°C. Digested mucin broth was filter-sterilized (0.5 μm pore size).

Succinate concentration measurement in digested mucin—The succinate concentration in digested mucin was measured using a coupled enzymatic assay according to the recommendations of the manufacturer. Freshly prepared solutions of pure succinate were used as a standard curve. Some biological samples were spiked with known amounts of pure succinate as controls.

Anaerobic growth of *S*. Tm in mucin broth—Fresh hog mucin broth (0.5 % mucin in NCE media) or filter-sterilized supernatant of *Bacteroides thetaiotaomicron*-digested mucin was inoculated with equal mixtures of the *Salmonella* Typhimurium *phoN* mutant (wild-type strain; AJB715) and the Δ*sdhA* mutant (SW1397), the Δ*sucAB* mutant (SW1285), the Δ*sucCD* mutant (SW1286), and the Δ*dcuA* Δ*dcuB* Δ*dctA* mutant (SW1411) or the Δ*sdhA* *phoN*::Kan^R mutant (SW1414) and the Δ*sdhA* Δ*dcuA* Δ*dcuB* Δ*dctA* mutant (SW1413) at a final concentration of 1×10^3 CFU/ml for each strain. Sodium nitrate or sodium tetrathionate were added at a final concentration of 40 mM, as indicated. After 18 h of anaerobic growth at 37°C, bacterial numbers we re determined by spreading serial ten-fold dilutions on selective LB agar plates.

Animal models of *S*. Tm-induced colitis

Streptomycin-treated mouse model: Groups of 7–10 week old C57BL/6 mice received 20 mg per animal through the intragastric route. After 24 h, mice were intragastrically inoculated with 1×10^9 CFU for single strain infection experiments, 5×10^8 CFU of each strain for competitive infection experiments, or mock treated (LB broth). For the experiments shown in Fig. 1, groups of mice were infected with equal mixtures of AJB715 and SW1056 as well as SW1401 and SW1203. For the experiments shown in Fig. 2, groups of animals were infected with IR715 or SPN487. For the experiments shown in Fig. 3, groups of mice were infected with equal mixtures of AJB715 and SW1397. In some experiments, animals were orally treated with tributyrin (5 g/kg) 3 h post infection or mock-treated with PBS (Rivera-Chavez et al., 2016). Two, three, and four days after infection, samples for histopathology, flash frozen cecal and colonic tissue for RNA and protein extraction, and cecal and colonic luminal material (*S*. Tm colonization) were collected, as indicated. In some experiments, luminal content was flash frozen (liquid nitrogen) for bacterial gene expression analyses.

CBA colitis model: Groups of 8–10 week old CBA mice were intragastrically infected with 1×10^9 CFU for single strain infection experiments, 5×10^8 CFU of each strain for competitive infection experiments, or mock treated (LB broth). After 7 days, samples were collected as described above. For the experiments shown in Fig. 4A and B, mice were infected with AJB715 and SW1285, AJB715 and SW1286, AJB715 and SW1288, AJB715 and SW1056, SW1401 and SW1203, SW1410 and SW1397, respectively. For the experiments shown in Fig. 4C–F, groups of animals were inoculated with IR715 and SW1397, respectively. For Fig. 5A–C, groups of animals were infected with AJB715 and

SW1397, AJB715 and SW1411, or SW1410 and SW1413. For Fig. 5C–E, groups of animals were infected with IR715, SW1411, or mock-treated.

Germ-free and conventionally-raised Swiss Webster mice: 6–8 week old germ-free mice were intragastrically inoculated with 3×10^9 CFU of *Bacteroides thetaiotaomicron*. After 3 days, mono-associated and germ-free control animals were infected with an equal mixture of AJB715 and SW1411, SW1410 and SW1413, or AJB715 and SW1397 as described above. Furthermore, cecal microbiota from one CBA donor mouse was orally transferred to a germ-free Swiss Webster breeder pair, which was then maintained under conventional housing conditions. Offspring from this breeder pair was used for the experiment shown in Fig. S5C.

Quantification of inflammatory markers by RT-qPCR—Relative mRNA levels of *Nos2*, *Cxcl1*, and *Tnfa* was determined by RT-qPCR as described previously (Winter et al., 2009). Briefly, tissue was homogenized in a Mini beadbeater (Biospec Products) and RNA was extracted using the TRI reagent method. cDNA was generated by TaqMan reverse transcription reagents. Real-time PCR was performed using SYBR Green qPCR master mix. Data was acquired in a QuantStudio 6 Flex instrument (Life Technologies) and analyzed using the comparative Ct method. Target gene transcription of each sample was normalized to *Gapdh* mRNA levels.

Bacterial gene expression—To determine bacterial gene expression *in vitro*, mucin broth was inoculated with 1×10^3 CFU/ml of *S*. Tm and anaerobically cultured at 37°C for 16 h. Sodium nitrate and tetra thionate was added at a concentration of 40 mM, as indicated. RNA was extracted using the Aurum Total RNA Mini Kit. To investigate bacterial gene expression in the intestinal content, flash frozen cecal material in TRI reagent was homogenized for 1 min in a bead beater (BioSpec) and RNA isolated using the TRI reagent method. RT-PCR and qPCR were performed as described above. Gene expression was normalized to *S*. Tm 16S rRNA levels. A mock-RT-PCR, lacking reverse transcriptase, was performed for each sample and gene of interest to control for DNA contamination.

Histopathology—Cecal and colonic tissue was fixed in phosphate-buffered formalin for 48 h and embedded in paraffin. Sections (5 μm) were stained with hematoxylin and eosin. Stained sections were blinded and evaluated by a veterinary pathologist according to the criteria listed in the supplementary material. The contrast for the images was uniformly (linear) adjusted using Photoshop CS6.

iNOS expression in intestinal tissue by Western Blot—After murine colonic tissue homogenization with a Mini-BeadBeater (BioSpec Products), colonic proteins were extracted with TRI Reagent according to the manufacturer's specifications (Molecular Research Center). Precipitated proteins were resuspended in a 1 % w/v sodium dodecyl sulfate (SDS) and 10 mM β-mercaptoethanol solution. Protein concentration of each sample was calculated based on the absorbance at 280 nm measured with an Epoch Microplate Spectrophotometer (BioTek Instruments). Samples were boiled for 1 min and then 10 μg of each sample were resolved by 10% SDS-PAGE. Proteins were transferred to polyvinylidene fluoride (PVDF) membranes (Millipore Immobilon-P) by wet transfer (Bio-Rad Laboratories). Membranes were blocked in 3 % non-fat dry milk and 0.1 % Tween 20 in

phosphate-buffered saline (pH 7.4) solution. To detect tubulin and inducible nitric oxide synthase (iNOS) expression, membranes were incubated overnight with primary antibodies. Horseradish peroxidase-conjugated antibodies were used as secondary antibodies. A G:Box imaging system (Syngene) was used to detect the secondary antibodies after 1 min incubation with Immobilon Western Substrate. Images were processed with Photoshop CS6 (Adobe) to uniformly adjust brightness levels.

Metabolite profiling and quantification of succinate—Colon and cecal content from mice was collected in sterile PBS. Samples were agitated for 2 min and debris and bacterial cells were removed by centrifugation at 6,000 g for 15 min at 4°C. For *in vitro* bacterial cultures, 2 ml of culture were centrifuged at 20,000 g at 4°C. The supernatant was removed and su ccinic-2,2,3,3,-d_4 acid was added as an internal control. Samples were dried using a SpeedVac concentrator (Eppendorf) for 2 h and stored at −80°C. External standards and biological samples were derivatized as follows: After adding 0.1 ml of water-free pyridine, each sample was sonicated for 1 min and incubated for 20 min at 80°C. Then 0.1 ml of *N*-*tert*-Butyldimethylsilyl-*N*-methyltrifluoroacetamide with 1 % *tert*-Butyldimethylchlorosilane was added to the samples and incubated at 80°C for 1 h. After centrifugation at 20,000 g, derivatized samples were transferred to autosampler vials for gas chromatography-mass spectrometry (GC-MS) analysis (Shimadzu, TQ8040). The injection temperature was 250°C and the injection split ratio was set to 1:50 with an injection volume of 1 μl. The oven temperature started at 50°C for 2 min, increasing to 100°C at 2 0°C per min and to 330°C at 40°C per min with a final hold at this temperature for 3 min. Flow rate of the helium carrier gas was kept constant at a linear velocity of 50 cm/s. The column used was a 30 m × 0.25 mm × 0.25 μm Rtx-5Sil MS (Shimadzu). The interface temperature was 300°C. The electron impact ion sour ce temperature was 200°C, with 70 V ionization voltage and 150 μA current. For qualitative experiments, Q3 scans (range of 50–550 m/z, 1000 m/z per second) were performed. The retention time for succinate and deuterated succinate was 10.877 and 10.868 minutes respectively. Multiple reaction monitoring mode was used to quantitatively measure succinate and deuterated succinate, target ion m/z 289>147 reference ion m/z 331>189, and target ion m/z 293>147 reference ion m/z 335>189, respectively.

Transcriptional profile of *S*. Tm in the large intestine—Gnotobiotic Swiss Webster mice were orally inoculated with 1×10^5 CFU of AJB715 for 48 h as described above. Cecal content was collected and stored in RNALater at −80°C until further processing. Total RNA was extrac ted and cleaned using RNeasy PowerMicrobiome kit and RNeasy Purification kit (Qiagen, MD) according to the recommendations of the manufacturer. RNAseq library was constructed using TruSeq Stranded Total RNA Library Prep kit (Illumina, CA) and the resulting cDNA library was analyzed using TapeStation 4200 (Agilent, CA). Single-end 150 bp sequencing was conducted on an Illumina NextSeq system (Illumina, CA). RNAseq reads were trimmed and decontaminated using BBmap software suite. Reads that failed to align to mouse genome were mapped to the *S.* Tm LT2 genome using Bowtie2 (Langmead and Salzberg, 2012). Number of reads of each gene was determined using the Subread package (Liao et al., 2014). Relative expression of genes was determined, grouped into indicated pathways, and compared to previously published data (Kroger et al., 2013). The Bray-Curtis distances between samples was calculated using R Vegan packages implemented through

Qiime (Caporaso et al., 2010) and visualized via Emperor (Vazquez-Baeza et al., 2013). The RNAseq dataset was deposited at the European Nucleotide Archive under accession number PRJEB21324.

QUANTIFICATION AND STATISTICAL ANALYSIS

Statistical analysis—Statistical data analysis was performed using Graphpad PRISM. Succinate concentrations, fold changes in mRNA transcription, competitive indices, and abundance of *Salmonella* (CFU/g) underwent logarithmic transformation prior to descriptive and inferential statistical analysis. All transformed data was normally distributed, as determined by D'Agostino-Pearson normality test for large group sizes and Shapiro-Wilk for smaller sizes. The statistical significance of differences between groups was determined using the parametric Student's *t*-test applied to the log-transformed, normally distributed data. Cumulative histopathology scores did not follow a normal distribution and thus were analyzed using the non-parametric Mann-Whitney *U* test. Unless indicated otherwise, *, $P < 0.05$; **, $P < 0.01$; ***, $P < 0.001$; and ns, not statistically significant. Unless indicated otherwise in the figure legend, bars represent the geometric mean +/− standard error. When displaying aggregate data from mouse experiments, the number of animals per group (N) is indicated above each graph or in the figure legend. Animals that had to be euthanized for humane reasons prior to reaching the predetermined time point were excluded from the analysis.

DATA AND SOFTWARE AVAILABILITY

The accession number for the RNAseq data reported in this paper is PRJEB21324 at the European Nucleotide Archive.

KEY RESOURCES TABLE

REAGENT or RESOURCE	SOURCE	IDENTIFIER
Antibodies		
Anti-rabbit alpha/beta-tubulin	Cell Signaling Technology	Cat# 2148S
Anti-mouse iNOS	Becton Dickinson	Cat# 610431
Anti-rabbit peroxidase-conjugated	Bio-Rad Laboratories	Cat# 170-6515
Anti-mouse peroxidase-conjugated	Bio-Rad Laboratories	Cat# 170-6516
Bacterial and Virus Strains		
E. coli, DH5α λ*pir, F*⁻ *endA1 hsdR17 (r*⁻*m*⁺*) supE44 thi-1 recA1 gyrA relA1* Δ*(lacZYA-argF)U189 Φ80lacZΔM15* λ*pir*	Pal et al., 2005	DH5α λ*pir*
E. coli, S17-1 λ*pir, zxx*::RP4 2-(Tet^R::Mu) (Kan^R::Tn7) λ*pir recA1 thi pro hsdR* (r⁻m⁺)	Simon et al., 1983	S17-1 λ*pir*
S. Typhimurium, IR715 ATCC14028 Nal^R	Stojiljkovic et al., 1995	IR715
S. Typhimurium, SL1344 Strep^R	Hoiseth and Stocker, 1981	SL1344
S. Typhimurium, IR715 *phoN*::Kan^R	Kingsley et al., 2003	AJB715
S. Typhimurium, IR715 Δ*invA*::Tet^R Δ*spiB*::Kan^R	Raffatellu et al., 2009	SPN452
S. Typhimurium, IR715 Δ*invA*(*−9 to +2057*) Δ*spiB*(*+25 to +1209*)	Rivera-Chavez et al., 2013	SPN487

REAGENT or RESOURCE	SOURCE	IDENTIFIER
S. Typhimurium, ATCC14028 Δ*sdhA*::Kan^R	Porwollik et al., 2014	STM0734
S. Typhimurium, SL1344 Δ*sdhA*	This study	MW156
S. Typhimurium, SL1344 Δ*invA*::Tet^R Δ*spiB*::Kan^R	This study	MW231
S. Typhimurium, SL1344 Δ*invA*::Tet^R Δ*spiB*::Kan^R *phoN*::Cm^R	This study	MW251
S. Typhimurium, SL1344 Δ*invA*::Tet^R Δ*spiB*::Kan^R Δ*sdhA*	This study	MW256
S. Typhimurium, SL1344 *phoN*::Cm^R	Winter et al., 2014	SW759
S. Typhimurium, IR715 Δ*sdhA*::Kan^R	This study	SW1056
S. Typhimurium, IR715 Δ*invA* Δ*spiB* Δ*sdhA*::Kan^R	This study	SW1203
S. Typhimurium, IR715 Δ*sucAB*	This study	SW1285
S. Typhimurium, IR715 Δ*sucCD*	This study	SW1286
S. Typhimurium, IR715 Δ*aceAB*	This study	SW1288
S. Typhimurium, IR715 Δ*sdhA*	This study	SW1397
S. Typhimurium, IR715 Δ*invA* Δ*spiB phoN*::Kan^R	This study	SW1401
S. Typhimurium, IR715 Δ*sdhA phoN::sdhA*	This study	SW1410
S. Typhimurium, IR715 Δ*dcuA* Δ*dcuB* Δ*dctA*	This study	SW1411 (Δ3)
S. Typhimurium, IR715 Δ*dcuA* Δ*dcuB* Δ*dctA* Δ*sdhA*::Kan^R	This study	SW1413
S. Typhimurium, IR715 Δ*sdhA phoN*::Kan^R	This study	SW1414
B. thetaiotaomicron, VPI 5482 Δ*tdk*	Koropatkin et al., 2008	VPI 5482 Δ*tdk*
B. thetaiotaomicron, Δ*tdk* Δ*frdCAB*	This study	MW399
Biological Samples		
Chemicals, Peptides, and Recombinant Proteins		
Gibson Assembly Master Mix	NEB	Cat# E2611L
LB Broth, Miller (Luria Bertani)	Becton Dickinson	Cat# 244520
LB Agar, Miller (Luria Bertani)	Becton Dickinson	Cat# 244620
Bacto Brain Heart Infusion	Becton Dickinson	Cat# 237500
Sheep Blood	Hemostat	Cat# DSB1
Columbia Agar	Sigma	Cat# 27688
Bacto Tryptone	Becton Dickinson	Cat# 211705
Sodium Nitrate	Sigma	Cat# S5506
Sodium Tetrathionate	Sigma	Cat# P2926
5-fluoro-2′-deoxyuridine (FUdR)	ARK Pharm	Cat# AK-24802-1
Mucin from porcine stomach, Type II	Sigma-Aldrich	Cat# M2378
TRI Reagent	Molecular Research	Cat# TR118
TaqMan Reverse Transcription Reagents	Life Technologies	Cat# N8080234
SYBR Green qPCR Master Mix	Life Technologies	Cat# 4309155
Succinic-2,2,3,3,-d4 acid	CDN Isotopes	Cat# D-197

REAGENT or RESOURCE	SOURCE	IDENTIFIER
Pyridine anhydrous	Sigma	Cat# 270970
MTBSTFA (with 1% t-BDMCS)	Sigma	Cat# M-108
Critical Commercial Assays		
Succinic acid enzymatic assay	Megazyme	Cat# K-SUCC
Aurum Total RNA Mini Kit	BioRad	Cat# 7326820
PowerMicrobiome RNA Isolation Kit	MoBio	Cat# 26000-50
RNeasy Purification kit	Qiagen	Cat# 74204
TruSeq Stranded Total RNA Library Prep kit	Illumina	Cat# RS-122-2201
Tributyrin	Sigma	Cat# W222305
Immobilon Western Chemiluminescent HRP Substrate	Millipore	Cat# WBKLS0500
Deposited Data		
Salmonella in vivo RNAseq dataset	European Nucletide Archive	PRJEB21324
Salmonella transcriptomic compendium from Kroger *et al.*, 2013 (http://bioinf.gen.tcd.ie/cgi-bin/salcom.pl?_HL)	GEO database	GSE49829
Experimental Models: Cell Lines		
Experimental Models: Organisms/Strains		
C57BL/6 WT	Jackson Laboratory	Cat# 000664
C57BL/6 *Cybb*$^{-/-}$	Jackson Laboratory	Cat# 002365
C57BL/6 *Nos2*$^{-/-}$	Jackson Laboratory	Cat# 002609
CBA/J	Jackson Laboratory	Cat# 000656
Swiss Webster, ex Germ-Free colonized with CBA/J microbiota	This study	N/A
Germ-free Swiss-Webster	Hooper Lab	N/A
Oligonucleotides		
Primer used in this study, see Table S1	This paper	N/A
Recombinant DNA		
Plasmid: pExchange-*tdk, ori*(R6K) *mobRP4 tdk* Carb^{R} Erm^{R}	Koropatkin et al., 2008	pExchange-*tdk*
Plasmid: pGP704, *ori*(R6K) *mobRP4* Carb^{R}	Miller and Mekalanos, 1988	pGP704
Plasmid: pRDH10, *ori*(R6K) *mobRP4 sacRB* Cm^{R} Tet^{R}	Kingsley et al., 1999	pRDH10
Plasmid: Up- and downstream region of *sucAB* in pRDH10	This study	pSW284
Plasmid: Up- and downstream region of *sucCD* in pRDH10	This study	pSW286
Plasmid: Up- and downstream region of *aceAB* in pRDH10	This study	pSW288
Plasmid: Up- and downstream region of *sdhA* in pRDH10	This study	pSW306

REAGENT or RESOURCE	SOURCE	IDENTIFIER
Plasmid: Internal fragment of the *phoN* coding sequence cloned into pGP704	This study	pSW327
Plasmid: *sdhA* promoter and coding sequence cloned into pSW327	This study	pSW328
Plasmid: Up- and downstream region of *dctA* in pRDH10	This study	pSW299
Plasmid: Up- and downstream region of *dcuA* in pRDH10	This study	pSW300
Plasmid: Up- and downstream region of *dcuB* in pRDH10	This study	pSW301
Plasmid: Up- and downstream region of *frdCAB* in pExchange-*tdk*	This study	pMW5
Software and Algorithms		
Prism 7	GrapPad Software	https://www.graphpad.com/scientific-software/pris
TapeStation 4200	Agilent, CA	
BBmap software suite		http://jgi.doe.gov/data-and-tools/bbtools/
Bowtie2	Langmead and Salzberg, 2012	http://bowtie-bio.sourceforge.net/bowtie2/index.sht
R Vegan		https://cran.r-project.org/web/packages/vegan/inde
Qiime	Caporaso et al., 2010	http://qiime.org
Emperor	Vazquez-Baeza et al., 2013	https://biocore.github.io/emperor/
GCMS Real Time Analysis	Shimadzu, TQ8040	N/A
Photoshop CS6	Adobe Photoshop	N/A
G:Box Imaging System	Syngene	N/A
Other		

Supplementary Material

Refer to Web version on PubMed Central for supplementary material.

Acknowledgments

Work in SEW's lab was funded by the NIH (AI118807, AI103248, AI128151) and The Welch Foundation (I-1858). Work in LVH's lab was funded by the NIH (DK070855), the Welch Foundation (I-1874) and the Howard Hughes Medical Institute. JK is supported by the Cancer Prevention and Research Institute of Texas (grant RP150596). The funders had no role in study design, data collection and interpretation, or the decision to submit the work for publication. Any opinions, findings, and conclusions or recommendations expressed in this material are those of the author(s) and do not necessarily reflect the views of the funding agencies. We would like to thank Drs. David Hendrixson, Julie Pfeiffer, and Vanessa Sperandio for helpful discussion and Madeline Smoot for technical assistance.

References

Ali MM, Newsom DL, Gonzalez JF, Sabag-Daigle A, Stahl C, Steidley B, Dubena J, Dyszel JL, Smith JN, Dieye Y, et al. Fructose-asparagine is a primary nutrient during growth of Salmonella in the inflamed intestine. PLoS pathogens. 2014; 10:e1004209. [PubMed: 24967579]

Alteri CJ, Himpsl SD, Engstrom MD, Mobley HL. Anaerobic respiration using a complete oxidative TCA cycle drives multicellular swarming in Proteus mirabilis. mBio. 2012; 3

Amarasingham CR, Davis BD. Regulation of alpha-ketoglutarate dehydrogenase formation in Escherichia coli. The Journal of biological chemistry. 1965; 240:3664–3668. [PubMed: 5319784]

Barman M, Unold D, Shifley K, Amir E, Hung K, Bos N, Salzman N. Enteric salmonellosis disrupts the microbial ecology of the murine gastrointestinal tract. Infection and immunity. 2008; 76:907–915. [PubMed: 18160481]

Barthel M, Hapfelmeier S, Quintanilla-Martinez L, Kremer M, Rohde M, Hogardt M, Pfeffer K, Russmann H, Hardt WD. Pretreatment of mice with streptomycin provides a Salmonella enterica serovar Typhimurium colitis model that allows analysis of both pathogen and host. Infection and immunity. 2003; 71:2839–2858. [PubMed: 12704158]

Caporaso JG, Kuczynski J, Stombaugh J, Bittinger K, Bushman FD, Costello EK, Fierer N, Pena AG, Goodrich JK, Gordon JI, et al. QIIME allows analysis of high-throughput community sequencing data. Nat Methods. 2010; 7:335–336. [PubMed: 20383131]

Coombes BK, Coburn BA, Potter AA, Gomis S, Mirakhur K, Li Y, Finlay BB. Analysis of the contribution of Salmonella pathogenicity islands 1 and 2 to enteric disease progression using a novel bovine ileal loop model and a murine model of infectious enterocolitis. Infection and immunity. 2005; 73:7161–7169. [PubMed: 16239510]

Crawford RW, Keestra AM, Winter SE, Xavier MN, Tsolis RM, Tolstikov V, Baumler AJ. Very long O-antigen chains enhance fitness during Salmonella-induced colitis by increasing bile resistance. PLoS pathogens. 2012; 8:e1002918. [PubMed: 23028318]

Cronan JE, Laporte D. Tricarboxylic Acid Cycle and Glyoxylate Bypass. EcoSal Plus. 2013; doi: 10.1128/ecosalplus.3.5.2

Crost EH, Tailford LE, Le Gall G, Fons M, Henrissat B, Juge N. Utilisation of mucin glycans by the human gut symbiont Ruminococcus gnavus is strain-dependent. PLoS One. 2013; 8:e76341. [PubMed: 24204617]

Cummings JH, Pomare EW, Branch WJ, Naylor CP, Macfarlane GT. Short chain fatty acids in human large intestine, portal, hepatic and venous blood. Gut. 1987; 28:1221–1227. [PubMed: 3678950]

Curtis MM, Hu Z, Klimko C, Narayanan S, Deberardinis R, Sperandio V. The gut commensal Bacteroides thetaiotaomicron exacerbates enteric infection through modification of the metabolic landscape. Cell host & microbe. 2014; 16:759–769. [PubMed: 25498343]

Cuskin F, Lowe EC, Temple MJ, Zhu Y, Cameron EA, Pudlo NA, Porter NT, Urs K, Thompson AJ, Cartmell A, et al. Human gut Bacteroidetes can utilize yeast mannan through a selfish mechanism. Nature. 2015; 517:165–169. [PubMed: 25567280]

Eilam O, Zarecki R, Oberhardt M, Ursell LK, Kupiec M, Knight R, Gophna U, Ruppin E. Glycan degradation (GlyDeR) analysis predicts mammalian gut microbiota abundance and host diet-specific adaptations. mBio. 2014; 5

El Kaoutari A, Armougom F, Gordon JI, Raoult D, Henrissat B. The abundance and variety of carbohydrate-active enzymes in the human gut microbiota. Nature reviews Microbiology. 2013; 11:497–504. [PubMed: 23748339]

Faber F, Thiennimitr P, Spiga L, Byndloss MX, Litvak Y, Lawhon S, Andrews-Polymenis HL, Winter SE, Baumler AJ. Respiration of Microbiota-Derived 1,2-propanediol Drives Salmonella Expansion during Colitis. PLoS pathogens. 2017; 13:e1006129. [PubMed: 28056091]

Ferreyra JA, Wu KJ, Hryckowian AJ, Bouley DM, Weimer BC, Sonnenburg JL. Gut microbiota-produced succinate promotes C. difficile infection after antibiotic treatment or motility disturbance. Cell host & microbe. 2014; 16:770–777. [PubMed: 25498344]

Fischbach MA, Sonnenburg JL. Eating for two: how metabolism establishes interspecies interactions in the gut. Cell host & microbe. 2011; 10:336–347. [PubMed: 22018234]

Flint HJ, Scott KP, Duncan SH, Louis P, Forano E. Microbial degradation of complex carbohydrates in the gut. Gut Microbes. 2012; 3:289–306. [PubMed: 22572875]

Galan JE, Curtiss R 3rd. Cloning and molecular characterization of genes whose products allow Salmonella typhimurium to penetrate tissue culture cells. Proceedings of the National Academy of Sciences of the United States of America. 1989; 86:6383–6387. [PubMed: 2548211]

Godinez I, Haneda T, Raffatellu M, George MD, Paixao TA, Rolan HG, Santos RL, Dandekar S, Tsolis RM, Baumler AJ. T cells help to amplify inflammatory responses induced by Salmonella enterica serotype Typhimurium in the intestinal mucosa. Infect Immun. 2008; 76:2008–2017. [PubMed: 18347048]

Gunn JS. The Salmonella PmrAB regulon: lipopolysaccharide modifications, antimicrobial peptide resistance and more. Trends Microbiol. 2008; 16:284–290. [PubMed: 18467098]

Gutnick D, Calvo JM, Klopotowski T, Ames BN. Compounds which serve as the sole source of carbon or nitrogen for Salmonella typhimurium LT-2. Journal of bacteriology. 1969; 100:215–219. [PubMed: 4898986]

Hapfelmeier S, Ehrbar K, Stecher B, Barthel M, Kremer M, Hardt WD. Role of the Salmonella pathogenicity island 1 effector proteins SipA, SopB, SopE, and SopE2 in Salmonella enterica subspecies 1 serovar Typhimurium colitis in streptomycin-pretreated mice. Infection and immunity. 2004; 72:795–809. [PubMed: 14742523]

Hapfelmeier S, Stecher B, Barthel M, Kremer M, Muller AJ, Heikenwalder M, Stallmach T, Hensel M, Pfeffer K, Akira S, et al. The Salmonella pathogenicity island (SPI)-2 and SPI-1 type III secretion systems allow Salmonella serovar typhimurium to trigger colitis via MyD88-dependent and MyD88-independent mechanisms. J Immunol. 2005; 174:1675–1685. [PubMed: 15661931]

Hensel M, Hinsley AP, Nikolaus T, Sawers G, Berks BC. The genetic basis of tetrathionate respiration in Salmonella typhimurium. Molecular microbiology. 1999; 32:275–287. [PubMed: 10231485]

Hensel M, Shea JE, Waterman SR, Mundy R, Nikolaus T, Banks G, Vazquez-Torres A, Gleeson C, Fang FC, Holden DW. Genes encoding putative effector proteins of the type III secretion system of Salmonella pathogenicity island 2 are required for bacterial virulence and proliferation in macrophages. Molecular microbiology. 1998; 30:163–174. [PubMed: 9786193]

Hoiseth SK, Stocker BA. Aromatic-dependent Salmonella typhimurium are non-virulent and effective as live vaccines. Nature. 1981; 291:238–239. [PubMed: 7015147]

Iuchi S, Lin EC. arcA (dye), a global regulatory gene in Escherichia coli mediating repression of enzymes in aerobic pathways. Proceedings of the National Academy of Sciences of the United States of America. 1988; 85:1888–1892. [PubMed: 2964639]

Kingsley RA, Humphries AD, Weening EH, De Zoete MR, Winter S, Papaconstantinopoulou A, Dougan G, Baumler AJ. Molecular and phenotypic analysis of the CS54 island of Salmonella enterica serotype typhimurium: identification of intestinal colonization and persistence determinants. Infection and immunity. 2003; 71:629–640. [PubMed: 12540539]

Kingsley RA, Reissbrodt R, Rabsch W, Ketley JM, Tsolis RM, Everest P, Dougan G, Baumler AJ, Roberts M, Williams PH. Ferrioxamine-mediated Iron(III) utilization by Salmonella enterica. Applied and environmental microbiology. 1999; 65:1610–1618. [PubMed: 10103258]

Koropatkin NM, Martens EC, Gordon JI, Smith TJ. Starch catabolism by a prominent human gut symbiont is directed by the recognition of amylose helices. Structure. 2008; 16:1105–1115. [PubMed: 18611383]

Koropatkin NM, Cameron EA, Martens EC. How glycan metabolism shapes the human gut microbiota. Nature reviews Microbiology. 2012; 10:323–335. [PubMed: 22491358]

Kroger C, Colgan A, Srikumar S, Handler K, Sivasankaran SK, Hammarlof DL, Canals R, Grissom JE, Conway T, Hokamp K, et al. An infection-relevant transcriptomic compendium for Salmonella enterica Serovar Typhimurium. Cell host & microbe. 2013; 14:683–695. [PubMed: 24331466]

Langmead B, Salzberg SL. Fast gapped-read alignment with Bowtie 2. Nat Methods. 2012; 9:357–359. [PubMed: 22388286]

Lawes M, Maloy S. MudSacI, a transposon with strong selectable and counterselectable markers: use for rapid mapping of chromosomal mutations in Salmonella typhimurium. Journal of bacteriology. 1995; 177:1383–1387. [PubMed: 7868615]

Lawley TD, Bouley DM, Hoy YE, Gerke C, Relman DA, Monack DM. Host transmission of Salmonella enterica serovar Typhimurium is controlled by virulence factors and indigenous intestinal microbiota. Infection and immunity. 2008; 76:403–416. [PubMed: 17967858]

Liao Y, Smyth GK, Shi W. featureCounts: an efficient general purpose program for assigning sequence reads to genomic features. Bioinformatics. 2014; 30:923–930. [PubMed: 24227677]

Liu JZ, Jellbauer S, Poe AJ, Ton V, Pesciaroli M, Kehl-Fie TE, Restrepo NA, Hosking MP, Edwards RA, Battistoni A, et al. Zinc sequestration by the neutrophil protein calprotectin enhances Salmonella growth in the inflamed gut. Cell host & microbe. 2012; 11:227–239. [PubMed: 22423963]

Lopez CA, Winter SE, Rivera-Chavez F, Xavier MN, Poon V, Nuccio SP, Tsolis RM, Baumler AJ. Phage-mediated acquisition of a type III secreted effector protein boosts growth of salmonella by nitrate respiration. mBio. 2012; 3

Lupp C, Robertson ML, Wickham ME, Sekirov I, Champion OL, Gaynor EC, Finlay BB. Host-mediated inflammation disrupts the intestinal microbiota and promotes the overgrowth of Enterobacteriaceae. Cell host & microbe. 2007; 2:119–129. [PubMed: 18005726]

Macy J, Probst I, Gottschalk G. Evidence for cytochrome involvement in fumarate reduction and adenosine 5′-triphosphate synthesis by Bacteroides fragilis grown in the presence of hemin. Journal of bacteriology. 1975; 123:436–442. [PubMed: 1150622]

Maier L, Vyas R, Cordova CD, Lindsay H, Schmidt TS, Brugiroux S, Periaswamy B, Bauer R, Sturm A, Schreiber F, et al. Microbiota-derived hydrogen fuels Salmonella typhimurium invasion of the gut ecosystem. Cell host & microbe. 2013; 14:641–651. [PubMed: 24331462]

Martens EC, Kelly AG, Tauzin AS, Brumer H. The devil lies in the details: how variations in polysaccharide fine-structure impact the physiology and evolution of gut microbes. J Mol Biol. 2014; 426:3851–3865. [PubMed: 25026064]

Meijer-Severs GJ, van Santen E. Short-chain fatty acids and succinate in feces of healthy human volunteers and their correlation with anaerobe cultural counts. Scand J Gastroenterol. 1987; 22:672–676. [PubMed: 3659829]

Mercado-Lubo R, Gauger EJ, Leatham MP, Conway T, Cohen PS. A Salmonella enterica serovar typhimurium succinate dehydrogenase/fumarate reductase double mutant is avirulent and immunogenic in BALB/c mice. Infection and immunity. 2008; 76:1128–1134. [PubMed: 18086808]

Mercado-Lubo R, Leatham MP, Conway T, Cohen PS. Salmonella enterica serovar Typhimurium mutants unable to convert malate to pyruvate and oxaloacetate are avirulent and immunogenic in BALB/c mice. Infection and immunity. 2009; 77:1397–1405. [PubMed: 19168732]

Miller VL, Mekalanos JJ. A novel suicide vector and its use in construction of insertion mutations: osmoregulation of outer membrane proteins and virulence determinants in Vibrio cholerae requires toxR. J Bacteriol. 1988; 170:2575–2583. [PubMed: 2836362]

Overbergh L, Giulietti A, Valckx D, Decallonne R, Bouillon R, Mathieu C. The use of real-time reverse transcriptase PCR for the quantification of cytokine gene expression. J Biomol Tech. 2003; 14:33–43. [PubMed: 12901609]

Pal D, Venkova-Canova T, Srivastava P, Chattoraj DK. Multipartite regulation of rctB, the replication initiator gene of Vibrio cholerae chromosome II. Journal of bacteriology. 2005; 187:7167–7175. [PubMed: 16237000]

Perrenoud A, Sauer U. Impact of global transcriptional regulation by ArcA, ArcB, Cra, Crp, Cya, Fnr, and Mlc on glucose catabolism in Escherichia coli. Journal of bacteriology. 2005; 187:3171–3179. [PubMed: 15838044]

Porwollik S, Santiviago CA, Cheng P, Long F, Desai P, Fredlund J, Srikumar S, Silva CA, Chu W, Chen X, et al. Defined single-gene and multi-gene deletion mutant collections in Salmonella enterica sv Typhimurium. PLoS One. 2014; 9:e99820. [PubMed: 25007190]

Prohl C, Wackwitz B, Vlad D, Unden G. Functional citric acid cycle in an arcA mutant of Escherichia coli during growth with nitrate under anoxic conditions. Archives of microbiology. 1998; 170:1–7. [PubMed: 9639597]

Pudlo NA, Urs K, Kumar SS, German JB, Mills DA, Martens EC. Symbiotic Human Gut Bacteria with Variable Metabolic Priorities for Host Mucosal Glycans. mBio. 2015; 6:e01282–01215. [PubMed: 26556271]

Rabin RS, Stewart V. Dual response regulators (NarL and NarP) interact with dual sensors (NarX and NarQ) to control nitrate- and nitrite-regulated gene expression in Escherichia coli K-12. Journal of bacteriology. 1993; 175:3259–3268. [PubMed: 8501030]

Raffatellu M, George MD, Akiyama Y, Hornsby MJ, Nuccio SP, Paixao TA, Butler BP, Chu H, Santos RL, Berger T, et al. Lipocalin-2 resistance confers an advantage to Salmonella enterica serotype Typhimurium for growth and survival in the inflamed intestine. Cell host & microbe. 2009; 5:476–486. [PubMed: 19454351]

Richardson AR, Payne EC, Younger N, Karlinsey JE, Thomas VC, Becker LA, Navarre WW, Castor ME, Libby SJ, Fang FC. Multiple targets of nitric oxide in the tricarboxylic acid cycle of Salmonella enterica serovar typhimurium. Cell host & microbe. 2011; 10:33–43. [PubMed: 21767810]

Rivera-Chavez F, Winter SE, Lopez CA, Xavier MN, Winter MG, Nuccio SP, Russell JM, Laughlin RC, Lawhon SD, Sterzenbach T, et al. Salmonella uses energy taxis to benefit from intestinal inflammation. PLoS pathogens. 2013; 9:e1003267. [PubMed: 23637594]

Rivera-Chavez F, Zhang LF, Faber F, Lopez CA, Byndloss MX, Olsan EE, Xu G, Velazquez EM, Lebrilla CB, Winter SE, et al. Depletion of Butyrate-Producing Clostridia from the Gut Microbiota Drives an Aerobic Luminal Expansion of Salmonella. Cell host & microbe. 2016; 19:443–454. [PubMed: 27078066]

Rogowski A, Briggs JA, Mortimer JC, Tryfona T, Terrapon N, Lowe EC, Basle A, Morland C, Day AM, Zheng H, et al. Glycan complexity dictates microbial resource allocation in the large intestine. Nat Commun. 2015; 6:7481. [PubMed: 26112186]

Rubinstein R, Howard AV, Wrong OM. In vivo dialysis of faeces as a method of stool analysis. IV. The organic anion component. Clin Sci. 1969; 37:549–564. [PubMed: 5359007]

Schell MA, Karmirantzou M, Snel B, Vilanova D, Berger B, Pessi G, Zwahlen MC, Desiere F, Bork P, Delley M, et al. The genome sequence of Bifidobacterium longum reflects its adaptation to the human gastrointestinal tract. Proceedings of the National Academy of Sciences of the United States of America. 2002; 99:14422–14427. [PubMed: 12381787]

Schmieger H. Phage P22-mutants with increased or decreased transduction abilities. Mol Gen Genet. 1972; 119:75–88. [PubMed: 4564719]

Schwarz WH, Zverlov VV, Bahl H. Extracellular glycosyl hydrolases from clostridia. Adv Appl Microbiol. 2004; 56:215–261. [PubMed: 15566981]

Shimizu T, Ohtani K, Hirakawa H, Ohshima K, Yamashita A, Shiba T, Ogasawara N, Hattori M, Kuhara S, Hayashi H. Complete genome sequence of Clostridium perfringens, an anaerobic flesh-eater. Proceedings of the National Academy of Sciences of the United States of America. 2002; 99:996–1001. [PubMed: 11792842]

Simon R, Priefer U, Puhler A. A Broad Host Range Mobilization System for In Vivo Genetic Engineering: Transposon Mutagenesis in Gram Negative Bacteria. Nature Biotechnology. 1983; 1:784–791.

Stecher B, Barthel M, Schlumberger MC, Haberli L, Rabsch W, Kremer M, Hardt WD. Motility allows S. Typhimurium to benefit from the mucosal defence. Cell Microbiol. 2008; 10:1166–1180. [PubMed: 18241212]

Stecher B, Robbiani R, Walker AW, Westendorf AM, Barthel M, Kremer M, Chaffron S, Macpherson AJ, Buer J, Parkhill J, et al. Salmonella enterica serovar typhimurium exploits inflammation to compete with the intestinal microbiota. PLoS biology. 2007; 5:2177–2189. [PubMed: 17760501]

Steeb B, Claudi B, Burton NA, Tienz P, Schmidt A, Farhan H, Maze A, Bumann D. Parallel exploitation of diverse host nutrients enhances Salmonella virulence. PLoS pathogens. 2013; 9:e1003301. [PubMed: 23633950]

Stojiljkovic I, Baumler AJ, Heffron F. Ethanolamine utilization in Salmonella typhimurium: nucleotide sequence, protein expression, and mutational analysis of the cchA cchB eutE eutJ eutG eutH gene cluster. Journal of bacteriology. 1995; 177:1357–1366. [PubMed: 7868611]

Tchawa Yimga M, Leatham MP, Allen JH, Laux DC, Conway T, Cohen PS. Role of gluconeogenesis and the tricarboxylic acid cycle in the virulence of Salmonella enterica serovar Typhimurium in BALB/c mice. Infection and immunity. 2006; 74:1130–1140. [PubMed: 16428761]

Thiennimitr P, Winter SE, Winter MG, Xavier MN, Tolstikov V, Huseby DL, Sterzenbach T, Tsolis RM, Roth JR, Baumler AJ. Intestinal inflammation allows Salmonella to use ethanolamine to compete with the microbiota. Proceedings of the National Academy of Sciences of the United States of America. 2011; 108:17480–17485. [PubMed: 21969563]

Turton LJ, Drucker DB, Ganguli LA. Effect of glucose concentration in the growth medium upon neutral and acidic fermentation end-products of Clostridium bifermentans, Clostridium sporogenes and peptostreptococcus anaerobius. J Med Microbiol. 1983; 16:61–67. [PubMed: 6822993]

Unden G, Kleefeld A. C4-Dicarboxylate Degradation in Aerobic and Anaerobic Growth. EcoSal Plus. 2004; 1

Vazquez-Baeza Y, Pirrung M, Gonzalez A, Knight R. EMPeror: a tool for visualizing high-throughput microbial community data. Gigascience. 2013; 2:16. [PubMed: 24280061]

Wilson RP, Raffatellu M, Chessa D, Winter SE, Tukel C, Baumler AJ. The Vi-capsule prevents Toll-like receptor 4 recognition of Salmonella. Cell Microbiol. 2008; 10:876–890. [PubMed: 18034866]

Wimpenny JW, Cole JA. The regulation of metabolism in facultative bacteria. 3. The effect of nitrate. Biochim Biophys Acta. 1967; 148:233–242. [PubMed: 4864932]

Winter SE, Thiennimitr P, Nuccio SP, Haneda T, Winter MG, Wilson RP, Russell JM, Henry T, Tran QT, Lawhon SD, et al. Contribution of flagellin pattern recognition to intestinal inflammation during Salmonella enterica serotype typhimurium infection. Infection and immunity. 2009; 77:1904–1916. [PubMed: 19237529]

Winter SE, Thiennimitr P, Winter MG, Butler BP, Huseby DL, Crawford RW, Russell JM, Bevins CL, Adams LG, Tsolis RM, et al. Gut inflammation provides a respiratory electron acceptor for Salmonella. Nature. 2010; 467:426–429. [PubMed: 20864996]

Winter SE, Winter MG, Poon V, Keestra AM, Sterzenbach T, Faber F, Costa LF, Cassou F, Costa EA, Alves GE, et al. Salmonella enterica Serovar Typhi conceals the invasion-associated type three secretion system from the innate immune system by gene regulation. PLoS pathogens. 2014; 10:e1004207. [PubMed: 24992093]

Winter SE, Winter MG, Xavier MN, Thiennimitr P, Poon V, Keestra AM, Laughlin RC, Gomez G, Wu J, Lawhon SD, et al. Host-derived nitrate boosts growth of E. coli in the inflamed gut. Science. 2013; 339:708–711. [PubMed: 23393266]

Wynosky-Dolfi MA, Snyder AG, Philip NH, Doonan PJ, Poffenberger MC, Avizonis D, Zwack EE, Riblett AM, Hu B, Strowig T, et al. Oxidative metabolism enables Salmonella evasion of the NLRP3 inflammasome. J Exp Med. 2014; 211:653–668. [PubMed: 24638169]

Xu J, Bjursell MK, Himrod J, Deng S, Carmichael LK, Chiang HC, Hooper LV, Gordon JI. A genomic view of the human-Bacteroides thetaiotaomicron symbiosis. Science. 2003; 299:2074–2076. [PubMed: 12663928]

HIGHLIGHTS

- During gut colonization, *S.* Typhimurium performs a complete, oxidative TCA cycle
- Host-derived alternative electron acceptors impact *S.* Tm central metabolism
- Uptake of C4-dicarboxylates enhances *S.* Tm fitness in the inflamed intestine
- Utilization of microbiota-derived succinate supports growth of *S.* Tm in the gut lumen

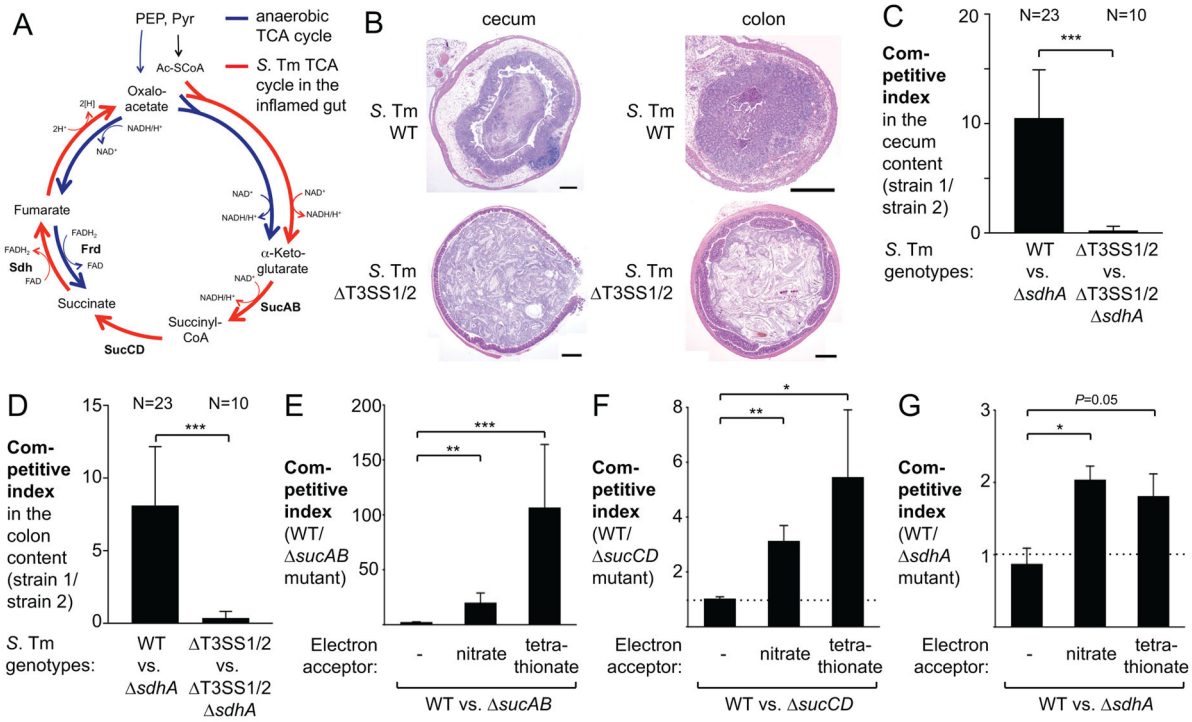

Figure 1. Contribution of succinate dehydrogenase to colonization in the streptomycin-treated mouse model

(A) Simplified model of the branched *S.* Tm TCA cycle under anaerobic conditions (blue arrows) and complete TCA in the inflamed gut. Frd, fumarate reductase; Sdh, succinate dehydrogenase; SucAB, α-ketoglutarate dehydrogenase; SucCD, succinyl-CoA synthetase. (B) Streptomycin-pretreated C57BL/6 mice were intragastrically inoculated with the *S.* Tm wild-type (WT) strain or a Δ*invA* Δ*spiB* (ΔT3SS1/2) mutant. Representative images of hematoxylin and eosin-stained sections of the cecum and the colon. Scale bar = 500 μm. (C – D) Streptomycin-pretreated C57BL/6 mice were intragastrically inoculated with an equal mixture of the indicated *S.* Tm strains. The competitive index in the cecal (C) and colonic content (D) was determined four days after infection. (E – F) Mucin broth was inoculated with an equal mixture of the *S.* Tm wild-type strain (WT) and a Δ*sucAB* mutant (E), a Δ*sucCD* mutant (F) or a Δ*sdhA* mutant (G) and the competitive index determined after 16 h of anaerobic growth in the absence or presence of nitrate (40 mM) and tetrathionate (40 mM). Bars represent geometric means ± standard error. *, $P < 0.05$; **, $P < 0.01$; ***, $P < 0.001$. The number of animals per group (N) is indicated above each bar. See also Fig. S1.

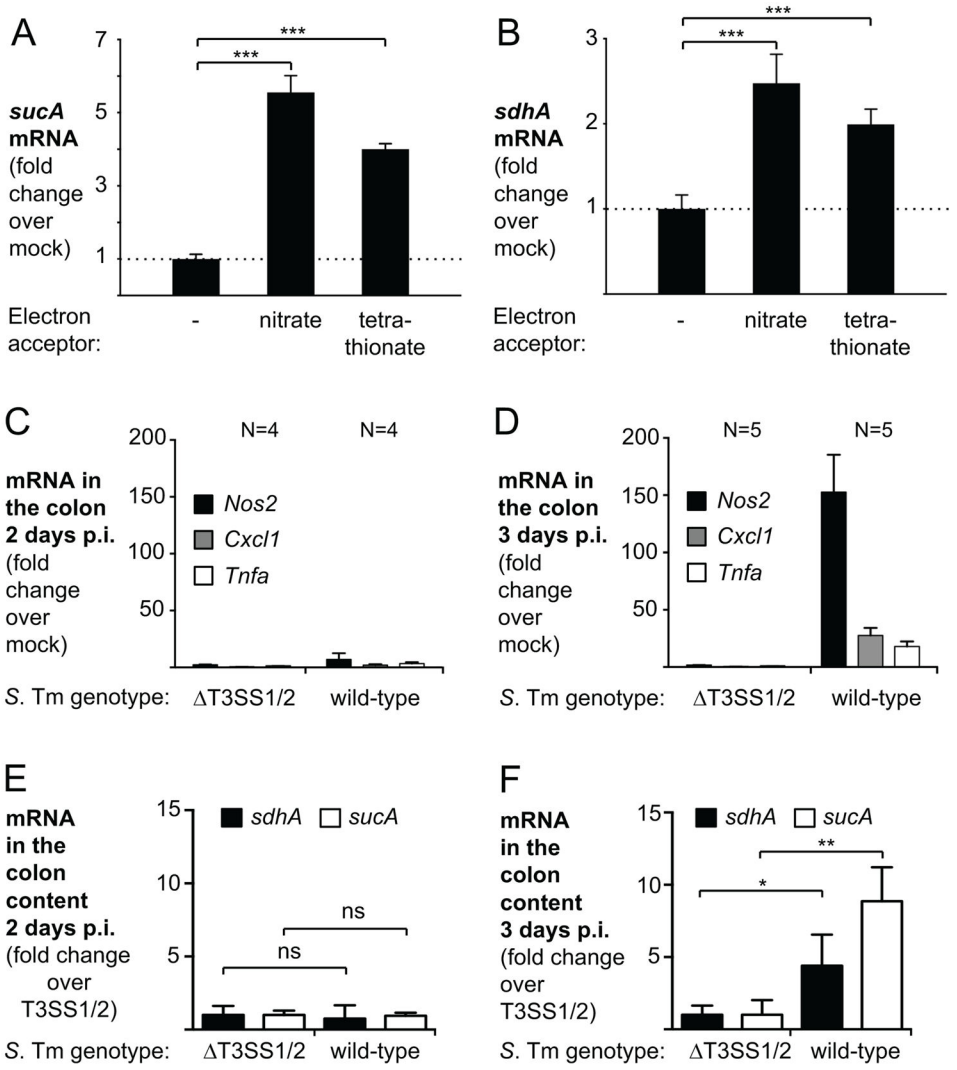

Figure 2. Effect of gut inflammation and electron acceptors on *sucA* and *sdhA* transcription

(A and B). Relative transcription of *sucA* (A) and *sdhA* (B) in mucin broth supplemented with the indicated electron acceptors was determined by RT-qPCR. Transcription of target genes was normalized to 16S rRNA. (C – D) Streptomycin-pretreated C57BL/6 mice were intragastrically inoculated with the *S.* Tm wild-type strain, an Δ*invA* Δ*spiB* (ΔT3SS1/2) mutant, or mock-treated (LB broth). (C and D) mRNA levels of *Nos2* (black bars), *Cxcl1* (gray bars), and *Tnfa* (white bars) in the colonic tissue was determined by RT-qPCR two days (C) and three days (D) post infection (p.i.). Transcription was normalized to *Gapdh* mRNA. (E and F) Bacterial RNA was extracted from the colon content. Relative transcription of *sdhA* (black bars) and *sucA* (white bars) normalized to *S.* Tm 16S rRNA was determined by RT-qPCR two (E) and three days (F) after infection. Bars represent geometric means ± standard error. *, $P < 0.05$; **, $P < 0.01$; ***, $P < 0.001$; ns, not statistically significant. The number of animals per group (N) is indicated above each bar. See also Fig. S2.

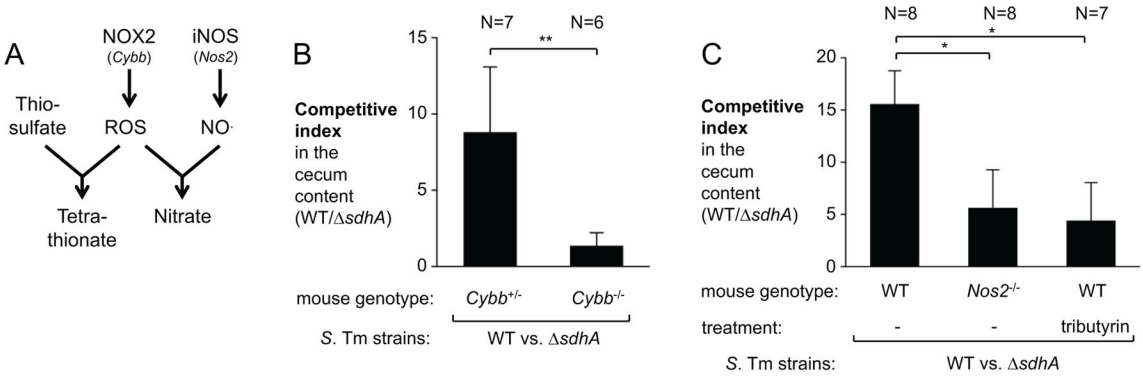

Figure 3. Impact of inflammation-derived electron acceptors on the TCA cycle during infection

(A) Simplified schematic outlining the contribution of NADPH oxidase 2 (NOX2) and inducible nitric oxide synthase (iNOS) to the generation of tetrathionate and nitrate via reactive oxygen species (ROS) and nitric oxide (NO). (B) Streptomycin-pretreated female *Cybb*$^{+/-}$ and *Cybb*$^{-/-}$ mice on the C57BL/6 background were intragastrically inoculated with the *S.* Tm wild-type strain and a Δ*sdhA* mutant. The competitive index in the cecal content was determined after four days. (C) Streptomycin-pretreated C57BL/6 wild-type mice and *Nos2*-deficient mice were inoculated with a mixture of the *S.* Tm wild-type strain and a Δ*sdhA* mutant. One group was treated with tributyrin as indicated. The competitive index in the cecal content was determined four days post infection. Bars represent geometric means ± standard error. *, $P < 0.05$; **, $P < 0.01$. The number of animals per group (N) is indicated above each bar.

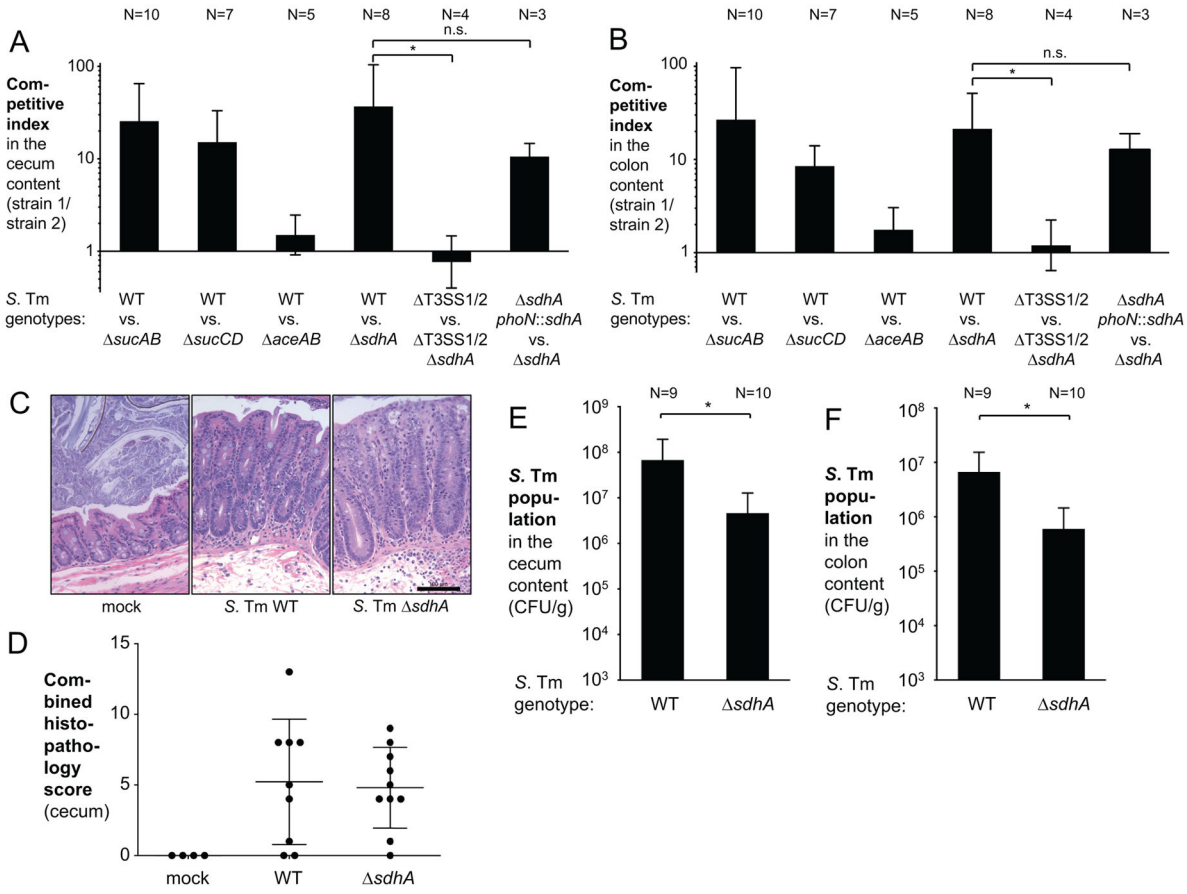

Figure 4. Sdh, α-ketoglutarate dehydrogenase, and succinyl-CoA synthetase activity contribute to fitness of *S.* Tm in mice with a native microbiota

(A – B) CBA mice were infected with an equal mixture of the indicated *S.* Tm strains by the intragastric route. Competitive index of the indicated strains in the cecal (A) and colonic lumen (B) 7 days after infection. WT, *S.* Tm wild-type strain; ΔT3SS1/2, Δ*invA* Δ*spiB* mutant. Bars represent geometric means ± standard error. *, $P < 0.05$; ns, not statistically significant. (C – F) CBA mice were intragastrically infected with the *S.* Tm wild-type strain or a Δ*sdhA* mutant. (C) Representative images of Hematoxylin and Eosin-stained cecal tissue. Scale bar equals 100 μm. (D) Combined histopathology score of pathological lesions in the cecum. Each dot represents one animal. The lines represent the mean ± standard error. (E and F) *S.* Tm population levels in the cecum (E) and colon (F) content 7 days after infection. Bars represent geometric means ± standard error. *, $P < 0.05$. The number of animals per group (N) is indicated above each bar. See also Fig. S3.

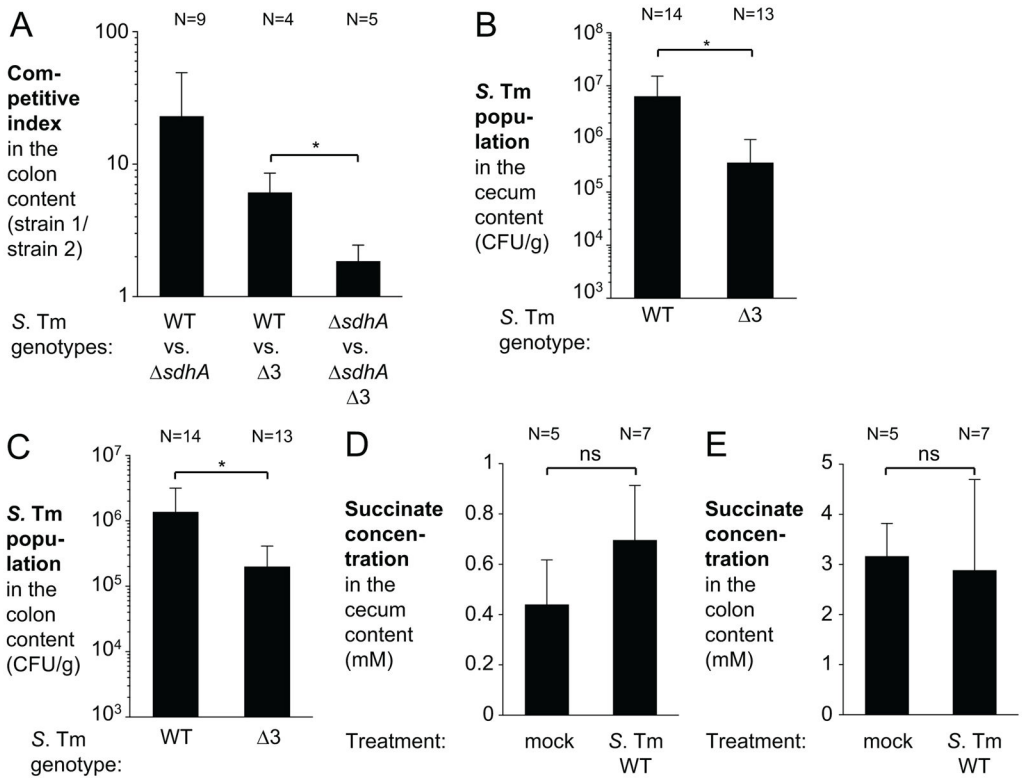

Figure 5. Succinate uptake and utilization confer a fitness advantage in competition with the native gut microbiota

(A) Groups of CBA mice were intragastrically infected with a mixture of the indicated *S.* Tm strains. Seven days after infection, the competitive index in the colon content was determined. Δ3, Δ*dcuA* Δ*dcuB* Δ*dctA* mutant. (B – E) As indicated, CBA mice were infected with the *S.* Tm wild-type strain (WT), the Δ3 mutant (Δ*dcuA* Δ*dcuB* Δ*dctA* mutant), or mock-treated. (B and C) *S.* Tm populations in the cecum (B) and colon content (C) 7 days after infection. (D and E) Succinate concentration in the cecum content (D) and colon content (E) as determined by GC/MS/MS. Bars represent geometric means ± standard error. *, $P < 0.05$; ns, not statistically significant. The number of animals per group (N) is indicated above each bar.

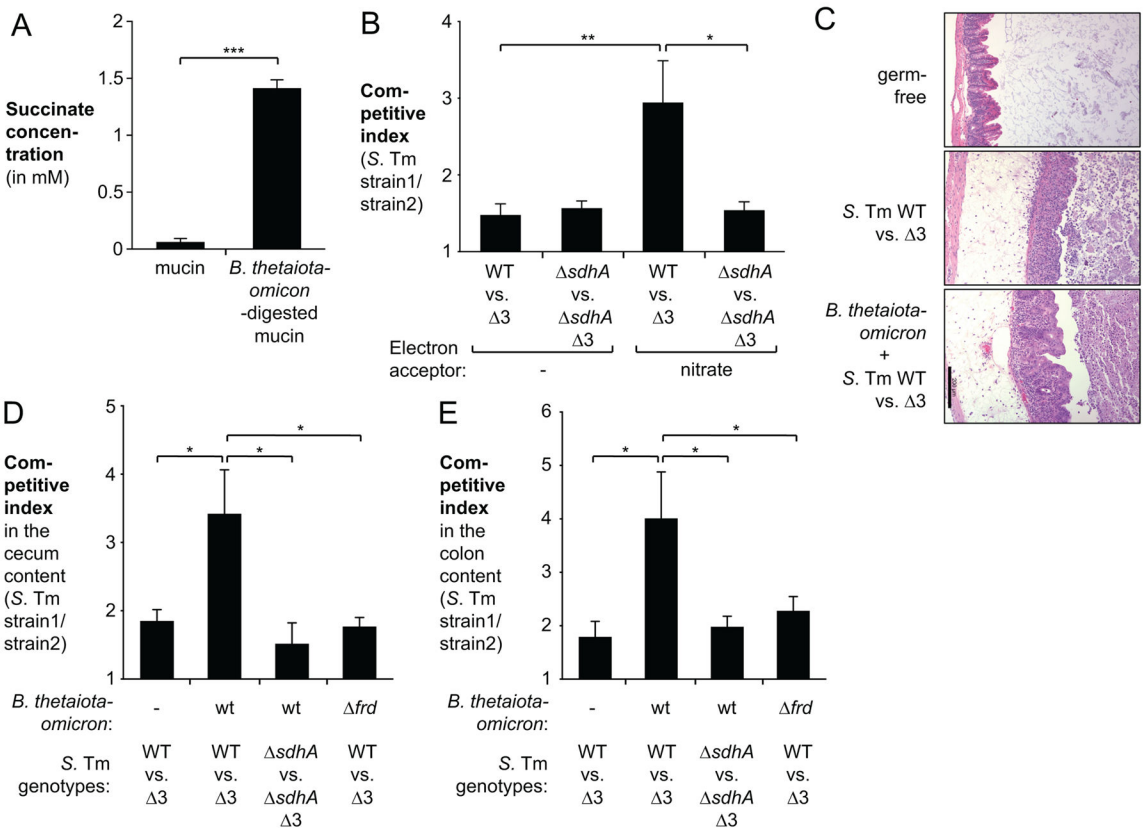

Figure 6. Microbiota-derived succinate enhances *S*. Tm growth during infection

(A – B) Mucin broth was inoculated with *B. thetaiotaomicron* and incubated anaerobically for 3 days. (A) Concentration of succinate in the supernatant (B) The filter-sterilized *B. thetaiotaomicron*-digested mucin broth was inoculated with the indicated *S*. Tm strains and the competitive index after 16 h of anaerobic growth determined. Sodium nitrate (40 mM) was added as indicated. (C – E) Germ-free Swiss Webster mice and mice mono-associated with the *B. thetaiotaomicron* wild-type strain (wt) or a Δ*frdCAB* (Δ*frd*) mutant were infected with an equal mixture of the *S*. Tm wild-type strain (WT) and the Δ*dcuA* Δ*dcuB* Δ*dctA* (Δ3) mutant or a mixture of a *S*. Tm Δ*sdhA* and a Δ*sdhA* Δ*dcuA* Δ*dcuB* Δ*dctA* (Δ*sdhA* Δ3) mutant. Samples were analyzed three days after infection. (C) Representative images of hematoxylin and eosin-stained sections of the cecum. Scale bar equals 200 μm. (D and E) Competitive index in the cecum (D) and colon content (E). Bars represent geometric means ± standard error. *, $P < 0.05$; **, $P < 0.01$; ***, $P < 0.001$. The number of animals per group (N) is indicated above each bar. See also Fig. S4–6.